Inorganic Chemistry

Article

pubs.acs.org/IC

New Water-Soluble Ruthenium(II) Terpyridine Complexes for Anticancer Activity: Synthesis, Characterization, Activation Kinetics, and Interaction with Guanine Derivatives

Ana Rilak,[†,‡] Ioannis Bratsos,*[,‡,§] Ennio Zangrando,[‡] Jakob Kljun,[∥,⊥] Iztok Turel,[∥] Živadin D. Bugarčić,[†] and Enzo Alessio*[,‡]

[†]Faculty of Science, University of Kragujevac, R. Domanovića 12, P.O. Box 60, 34000 Kragujevac, Serbia

[‡]Dipartimento di Scienze Chimiche e Farmaceutiche, Università di Trieste, Via L. Giorgieri 1, 34127 Trieste, Italy

[∥]Faculty of Chemistry and Chemical Technology, University of Ljubljana, Aškerčeva 5, SI-1000 Ljubljana, Slovenia

[⊥]EN→FIST Centre of Excellence, Dunajska 156, SI-1000 Ljubljana, Slovenia

Supporting Information

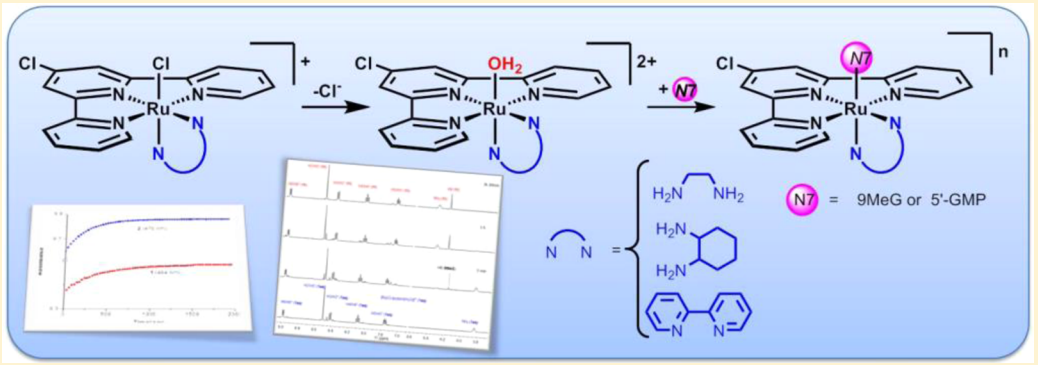

ABSTRACT: With the aim of assessing whether ruthenium(II) compounds with meridional geometry might be utilized as potential antitumor agents, a series of new, water-soluble, monofunctional ruthenium(II) complexes of the general formula *mer*-$[Ru(L_3)(N\text{-}N)X][Y]_n$ (where L_3 = 2,2′:6′,2″-terpyridine (tpy) or 4′-chloro-2,2′:6′,2″-terpyridine (Cl-tpy), N-N = 1,2-diaminoethane (en), 1,2-diaminocyclohexane (dach), or 2,2′-bipyridine (bpy); X = Cl or dmso-*S*; Y = Cl, PF_6, or CF_3SO_3; n = 1 or 2, depending on the nature of X) were synthesized. All complexes were fully characterized by elemental analysis and spectroscopic techniques (IR, UV/visible, and 1D and 2D NMR), and for three of them, i.e., [Ru(Cl-tpy)(bpy)Cl][Cl] ($\mathbf{3}_{Cl}$), [Ru(Cl-tpy)(en)(dmso-*S*)][Y]$_2$ [Y = PF_6 ($\mathbf{6}_{PF_6}$), CF_3SO_3 ($\mathbf{6}_{OTf}$)] and [Ru(Cl-tpy)(bpy)(dmso-*S*)][CF_3SO_3]$_2$ ($\mathbf{8}_{OTf}$), the X-ray structure was also determined. The new terpyridine complexes, with the exception of **8**, are well soluble in water (>25 mg/mL). ^{1}H and ^{31}P NMR spectroscopy studies performed on the three selected complexes [Ru(Cl-tpy)(N-N)Cl]$^+$ [N-N = en (**1**), dach (**2**), and bpy (**3**)] demonstrated that, after hydrolysis of the Cl ligand, they are capable of interacting with guanine derivatives [i.e., 9-methylguanine (9MeG) or guanosine-5′-monophosphate (5′-GMP)] through N7, forming monofunctional adducts with rates and extents that depend strongly on the nature of N-N: **1** ≈ **2** ≫ **3**. In addition, compound **1** shows high selectivity toward 5′-GMP compared to adenosine-5′-monophosphate (5′-AMP), in a competition experiment. Quantitative kinetic investigations on **1** and **2** were performed by means of UV/visible spectroscopy. Overall, the complexes with bidentate aliphatic diamines proved to be superior to those with bpy in terms of solubility and reactivity (i.e., release of Cl^- and capability to bind guanine derivatives). Contrary to the chlorido compounds, the corresponding dmso derivatives proved to be inert (viz., they do not release the monodentate ligand) in aqueous media.

INTRODUCTION

In the search for nonplatinum antitumor drugs with a different spectrum of activity and fewer side effects than those of cisplatin and its analogues, ruthenium compounds appear to be the front runners,[1] especially after the introduction of two ruthenium(III) complexes, namely, [indH]*trans*-[$RuCl_4$(ind)$_2$] (ind = indazole, KP1019) and [imH]*trans*-[$RuCl_4$(dmso-*S*)(im)] (im = imidazole, NAMI-A), into clinical trials.[2,3]

During the last decades, a large interest in ruthenium polypyridyl complexes as structure- and site-specific DNA binding agents with attractive photophysical properties has grown.[4,5] Studies on ruthenium polypyridyl complexes that feature at least one coordination site occupied by a good

Received: March 6, 2014
Published: June 2, 2014

   dx.doi.org/10.1021/ic5005215 | *Inorg. Chem.* 2014, 53, 6113−6126

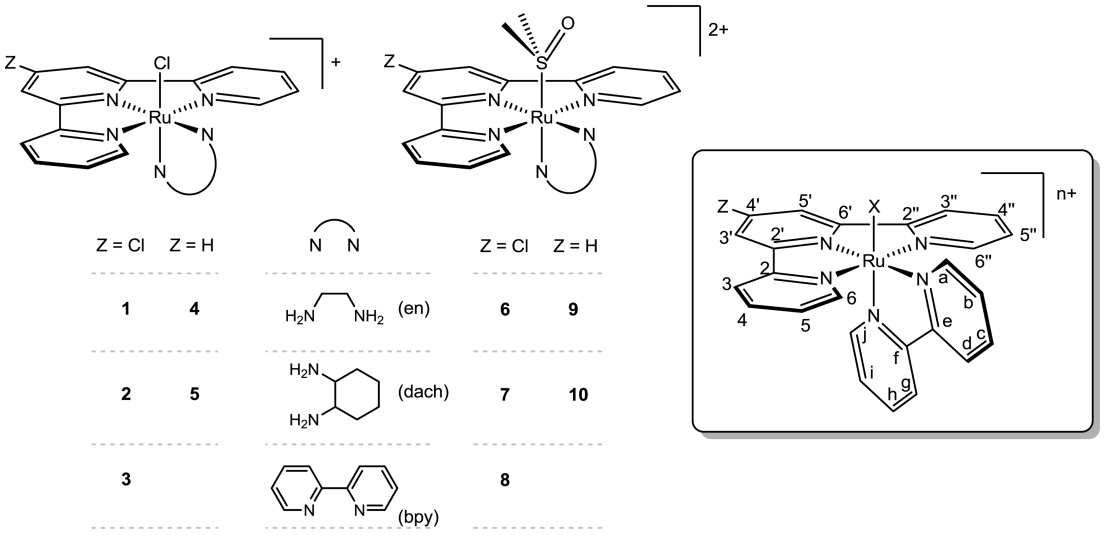

Figure 1. Schematic representation of complexes **1**−**10**. Inset: Numbering scheme of the tpy and bpy ligands used for the NMR characterization.

leaving group revealed that, besides being good intercalators, they can also coordinate DNA nucleobases in a two-step process, similar to cisplatin:[5] release of the labile ligand(s) with formation of the corresponding aqua species, followed by binding on nucleobases (*functional compounds*).[6] Some of them were found to possess also promising in vitro antitumor activity. For example, the complexes *mer*-[Ru(tpy)Cl_3] (tpy = 2,2′:6′,2″-terpyridine) and *α*-[Ru(azpy)$_2Cl_2$] (azpy = 2-phenylazopyridine) showed remarkably high cytotoxicity against most of the tested cell lines (with IC_{50} values in the low micromolar range).[7,8] In particular, the high activity of *mer*-[Ru(tpy)Cl_3] was assumed to derive from its ability to bind DNA through two guanine derivatives in a trans configuration, forming interstrand cross-links.[9] This hypothesis was supported by the observation that the monofunctional complex [Ru(tpy)(bpy)Cl][Cl] (bpy = 2,2′-bipyridine), which can also bind to DNA, displays a markedly lower activity than *mer*-[Ru(tpy)Cl_3].[7]

Over the past years, a number of monochloridoruthenium(II) terpyridine complexes of the type *mer*-[Ru(tpy)(N-N)Cl]$^+$, and/or their monoaqua analogues, containing different N-donor chelating ligands (N-N), such as bpy,[10] 4,4′-dimethyl-2,2′-bipyridine (Me_2bpy),[11] 4,4′-diphenyl-2,2′-dipyridine (biphbpy),[12] 1,10-phenanthroline (phen),[10,11] 3,4,7,8-tetramethyl-1,10-phenanthroline (tmephen),[12] dipyrido[3,2-*a*:2′,3′-*c*]phenazine (dppz),[10b,12] *N*,*N*,*N*′,*N*′-tetramethylethylenediamine (tmen),[10a,12] 2,2′-azobispyridine (apy),[13] azpy,[13b] and 2-phenylpyridinylmethyleneamine (impy),[13b] have been prepared and studied for their DNA binding ability. It is important to note that all of these complexes contain exclusively N-donor chelating ligands that are unable to form strong hydrogen bonds. It was found that most of the Ru^{II}-tpy complexes are capable to bind covalently to DNA (mainly at guanine residues) forming monofunctional adducts, and some of them to stop DNA replication.[7,12]

On the other hand, most of the recent research on anticancer ruthenium(II) compounds has been focused on half-sandwich organometallic ruthenium(II) species of the general formula [Ru(η^6-arene)(N-N)X][PF_6], known also as "piano-stool" compounds, which were found to possess promising activity both in vitro (with IC_{50} values ranging from 0.6 to 9 μM, depending on the arene and on the cell line) and in vivo, in particular when N-N is capable of making hydrogen bonds [e.g., N-N = 1,2-diaminoethane (en)].[14,15] Their activation is believed to require dissociation of the monodentate ligand X, i.e., X = Cl,[16] and thus they can be classified as *prodrugs* (or *functional compounds*), with a mechanism of action similar to that of platinum drugs. These monofunctional compounds bind preferentially to N7 of guanine in DNA, and the coordinative bond can be complemented by specific hydrogen-bonding interactions between the N−H of the chelating ligand and the carbonyl C6═O of guanine, as well as by intercalative binding of the arene.[17] These additional interactions result in unique modes of binding to duplex DNA and structural distortions that are distinctly different from those caused by cisplatin.[18] Therefore, the presence of a chelating ligand capable of acting as a hydrogen-bond donor, such as en, is believed to play a crucial role in the activity of piano-stool compounds.[17]

Recently, our group contributed to this field, developing a series of new half-sandwich ruthenium(II) *coordination compounds* structurally similar to the organometallic complexes, i.e., with a facial tridentate ligand in place of the arene (e.g., [9]aneS3 = 1,4,7-trithiacyclononane), a bidentate chelating ligand, and a labile entity.[19] We found that among the new series of complexes with the general formula [Ru([9]aneS3)(N-N)Cl][PF_6] only those with N-N = en or dach (dach = 1,2-diaminocyclohexane) showed moderate in vitro cytotoxicity, with IC_{50} values of ca. 80 μM (en) and 124 μM (dach) against the MDA-MB-231 breast carcinoma cell line.[19a−e] It is worth noting that these are the only compounds among those tested that fulfill simultaneously two important features: both are capable of hydrolyzing the chloride ligand at a reasonable rate (i.e., within minutes) and of acting as hydrogen-bond donors through the chelating ligand. Further studies on [Ru([9]aneS3)(en)Cl][PF_6] showed that this compound, similar to the organometallic analogues [Ru(η^6-arene)(en)Cl][PF_6], is capable of binding guanine derivatives through N7, forming monofunctional adducts after the relatively fast release of the Cl ligand. The coordinative binding is also assisted, as observed for the organometallic counterparts, by hydrogen bonding between the carbonyl of guanine and one NH of en, as evidenced by X-ray structural analysis in the case of [Ru([9]aneS3)(en)(9MeG-N7][PF_6]$_2$ (9MeG = 9-methylguanine).[20]

dx.doi.org/10.1021/ic5005215 | *Inorg. Chem.* 2014, 53, 6113−6126

Therefore, it appears that both *fac* and *mer* ruthenium(II) complexes of the general formula $[Ru(L_3)(N\text{-}N)X]^+$ (where L_3 is a tridentate ligand) are capable of making monofunctional adducts with DNA and of inducing cytotoxicity in cancer cells in vitro. However, despite some promising results, the solubility problems of terpyridine derivatives reduced the interest in the class of *mer* compounds, and they have been much less explored for anticancer activity compared to those with facial geometry.[7,9,11,13] It is therefore of interest in this context to obtain more insight at the molecular level on ruthenium complexes with the *mer* geometry.

In this work, building on the experience gained with half-sandwich ruthenium(II) coordination compounds, we investigated a series of *mer*-$[Ru(L_3)(N\text{-}N)X][Y]_n$ complexes in which L_3 is either tpy or Cl-tpy (4′-chloro-2,2′:6′,2″-terpyridine), X is a supposedly labile entity (X = Cl or dmso-*S*), N-N is a bidentate chelating ligand capable of hydrogen bonding with DNA nucleobases (N-N = en or dach), Y = Cl, PF_6, or CF_3SO_3, and n = 1 or 2, depending on the nature of X. We focused mainly on Cl-tpy derivatives because the Cl, as a hydrogen-bond acceptor, might be advantageous by forming additional hydrogen bonds, such as O−H···Cl, N−H···Cl, and C−H···Cl, with the hydrogen-bond donors of the proteins (for transportation) and DNA (for activity).[21] For comparative purposes, the corresponding Ru(Cl-tpy) complexes with N-N = bpy were also prepared and investigated. All new terpyridine complexes (Figure 1) were fully characterized by elemental analysis, IR, UV/visible, and 1D and 2D NMR spectroscopy. The molecular structures of three complexes, i.e., [Ru(Cl-tpy)(bpy)Cl][Cl] ($\mathbf{3}_{Cl}$), [Ru(Cl-tpy)(en)(dmso-*S*)][Y]$_2$ [Y = PF_6 ($\mathbf{6}_{PF_6}$) and CF_3SO_3 ($\mathbf{6}_{OTf}$)], and [Ru(Cl-tpy)(bpy)(dmso-*S*)][CF_3SO_3]$_2$ ($\mathbf{8}_{OTf}$), were determined also in the solid state by X-ray crystallography. The chemical behavior in aqueous solution of the new complexes and the binding properties of compounds **1**−**3** toward the guanine derivatives 9MeG and 5′-GMP (guanosine-5′-monophosphate), as model DNA bases, were investigated primarily by NMR spectroscopy in D_2O at ambient temperature. The relative affinity of 5′-GMP and 5′-AMP (adenosine-5′-monophosphate) toward complex **1** was also established by a competition experiment. The kinetics of the aquation of **1** and **2** and of the subsequent interaction with 9MeG and 5′-GMP were established quantitatively by UV/visible spectroscopy.

EXPERIMENTAL SECTION

Materials. 1,2-Diaminoethane (en), (±)-*trans*-1,2-diaminocyclohexane (dach), 2,2′-bipyridine (bpy), 4′-chloro-2,2′:6′,2″-terpyridine (Cl-tpy), 2,2′:6′,2″-terpyridine (tpy), 9-methylguanine (9MeG), guanosine-5′-monophosphate disodium salt hydrate (5′-GMP-Na_2), and adenosine-5′-monophosphate monohydrate (5′-AMP-H_2·H_2O) are commercially available and were used as received. The precursors *cis*-$[RuCl_2(dmso)_4]$,[22] $[Ru(tpy)Cl_3]$ (**P2**),[23] and $[Ru(tpy)Cl_2(dmso\text{-}S)]$ (**P4**)[24] were prepared as described in the literature, whereas the corresponding precursors $[Ru(Cl\text{-}tpy)Cl_3]$ (**P1**)[25] and $[Ru(Cl\text{-}tpy)Cl_2(dmso\text{-}S)]$ (**P3**)[21] were synthesized according to published procedures with some modifications and are reported in the Supporting Information (SI). All other chemicals were used as purchased without further purification.

Instrumental Methods. Monodimensional [^{1}H (500 MHz), ^{13}C (126 MHz), ^{31}P (202 MHz)] and bidimensional (^{1}H−^{1}H COSY, ^{1}H−^{13}C HSQC, ^{1}H−^{13}C HMBC) NMR spectra were recorded on a Varian 500 spectrometer. ^{1}H chemical shifts in D_2O were referenced to the internal standard 2,2-dimethyl-2,2-silapentane-5-sulfonate at δ 0.00 or to added 1,4-dioxane (δ 3.75), whereas in other solvents, they were referenced to the peak of a residual nondeuterated solvent [δ 4.33 for CD_3NO_2, 2.05 for $(CD_3)_2CO$, and 2.50 for dimethyl sulfoxide (DMSO)-d^6]; ^{13}C chemical shifts in D_2O were referenced to the peaks of traces of external solvents (δ 17.5 and 58.1 for ethanol and 39.4 for DMSO), whereas in other solvents, they were referenced to the peak of a residual nondeuterated solvent [δ 62.8 for CD_3NO_2, 29.84 for $(CD_3)_2CO$, and 39.52 for DMSO-d^6]. ^{31}P chemical shifts were referenced to an external 85% H_3PO_4 standard at 0.00 ppm. All NMR spectra were run at 298 K. The UV/visible spectra were obtained on a Jasco V-500 UV/visible spectrophotometer equipped with a Peltier temperature controller or on a PerkinElmer Lambda 35 double-beam spectrophotometer, using 1.0-cm-path-length quartz cuvettes (3.0 mL). IR spectra were recorded on a PerkinElmer 983G spectrometer. Elemental analysis was performed at the Dipartimento di Scienze e Tecnologie Chimiche, University of Udine (Italy).

Synthetic Procedures. In an attempt to isolate crystals suitable for X-ray analysis, most of the cationic complexes described below were synthesized with different counterions [either Cl^-, PF_6^-, or $CF_3SO_3^-$ (OTf^-)]; in such cases, only one preparation is reported here, whereas the others are detailed in the SI. Complexes that differ only in the nature of the counterion are labeled with the same number, as it is associated with the cation. When needed, the nature of the counterion is indicated as a subscript. The aqua species that are obtained in aqueous solution from some complexes upon hydrolysis of Cl^- are labeled with the same number of the parent compound followed by "aq". The NMR assignments of these species are reported in the SI.

General Synthetic Procedure for [Ru(Cl-tpy)(N-N)Cl][Cl] ($\mathbf{1}_{Cl}$−$\mathbf{3}_{Cl}$) and [Ru(tpy)(N-N)Cl][Cl] ($\mathbf{4}_{Cl}$ and $\mathbf{5}_{Cl}$). A weighed amount of **P1** was suspended in an ethanol/water (3:1) mixture containing 10 equiv of LiCl and 3 equiv of triethylamine (Et_3N) as a reductant. The chelating ligand N-N (1.2 equiv; N-N = en, dach, and bpy) was then added, and the mixture was refluxed for ca. 3 h under vigorous stirring. The violet-to-purple solution was filtered while hot to remove any undissolved material. Rotary concentration under reduced pressure to ca. $^1/_4$ of the initial volume and storage at 4.0 °C for 24 h induced formation of the product as a dark solid. It was collected by filtration, washed with ice-cold water, cold acetone, and diethyl ether, and vacuum-dried. The corresponding tpy complexes **4** and **5** were prepared with a similar procedure using **P2** as the starting material.

[Ru(Cl-tpy)(en)Cl][Cl] ($\mathbf{1}_{Cl}$). A total of 100.0 mg (0.210 mmol) of **P1**, 16.8 μL (0.252 mmol) of en, 89.0 mg (2.100 mmol) of LiCl, and 87.9 μL (0.630 mmol) of Et_3N in 20 mL of ethanol/water afforded **1** as a dark-purple solid. Yield: 70.6 mg (67%). Anal. Calcd for $C_{17}H_{18}Cl_3N_5Ru$ (499.79): C, 40.9; H, 3.63; N, 14.01. Found: C, 40.8; H, 3.71; N, 13.92. Complex **1** is soluble in water, methanol, and ethanol and slightly soluble in acetone and nitromethane, whereas it is insoluble in chloroform and dichloromethane. ^{1}H NMR (D_2O): δ 8.92 (d, 2H, J = 5.5 Hz, C6*H*/C6″*H*), 8.42 (s, 2H, C3′*H*/C5′*H*), 8.35 (d, 2H, J = 8.0 Hz, C3*H*/C3″*H*), 7.99 (t, 2H, J = 7.7 Hz, C4*H*/C4″*H*), 7.71 (ddd, 2H, J = 7.4, 5.6, and 1.3 Hz, C5*H*/C5″*H*), 5.71 (t br, 2H, J = 5.1 Hz, NH_2 en), 3.25 (m br, 2H, CH_2 en), 2.69 (s br, 2H, NH_2 en), 2.36 (m br, 2H, CH_2 en). ^{1}H NMR (CD_3NO_2): δ 8.95 (d, 2H, J = 5.5 Hz, C6*H*/C6″*H*), 8.42 (d, 2H, J = 8.1 Hz, C3*H*/C3″*H*), 8.38 (s, 2H, C3′*H*/C5′*H*), 8.06 (t, 2H, J = 7.6 Hz, C4*H*/C4″*H*), 7.73 (t, 2H, J = 6.3 Hz, C5*H*/C5″*H*), 5.34 (s br, 2H, NH_2 en), 3.48 (m br, 2H, CH_2 en), 2.62 (m br, 2H, CH_2 en), 2.02 (overlapped with the H_2O resonance, NH_2 en). ^{13}C NMR (CD_3NO_2): δ 162.4 (*C*2′/*C*6′), 160.8 (*C*2/*C*2″), 153.6 (*C*6H/*C*6″H), 137.6 (*C*4H/*C*4″H), 136.7 (*C*4′), 128.7 (*C*5H/*C*5″H), 124.4 (*C*3H/*C*3″H), 122.5 (*C*3′H/*C*5′H), 46.92 (*C*H$_2$ en), 46.91 (*C*H$_2$ en). Selected IR (KBr, cm^{-1}): ν_{NH} 3256 (m); ν_{tpy} 3036 (m), 1599 (s), 1474 (m), 1423 (s), 1119 (s), 787 (s), 566 (w); ν_{Ru-Cl} 320 (m). UV/visible spectrum [H_2O; λ_{max}, nm (ε, M^{-1} cm^{-1})]: 239 (24310), 277 (20993), 317 (29034), 370 (4375), 503 (4390), 562 (3830).

[Ru(Cl-tpy)(dach)Cl][Cl] ($\mathbf{2}_{Cl}$). A total of 100.0 mg (0.210 mmol) of **P1**, 30.3 μL (0.252 mmol) of dach, 89.0 mg (2.100 mmol) of LiCl, and 87.9 μL (0.630 mmol) of Et_3N in 20 mL of ethanol/water (3:1) afforded **2** as a dark-purple solid. Yield: 80.2 mg (69%). Anal. Calcd for $C_{21}H_{24}Cl_3N_5Ru$ (553.88): C, 45.5; H, 4.37; N, 12.64. Found: C, 45.4;

dx.doi.org/10.1021/ic5005215 | *Inorg. Chem.* 2014, 53, 6113−6126

H, 4.29; N, 12.72. Complex **2** is soluble in water, methanol, and ethanol and partially soluble in nitromethane, whereas it is insoluble in acetone, chloroform, and dichloromethane. ^{1}H NMR (D_2O): δ 8.98 (d, 1H, J = 5.1 Hz, C6*H*), 8.89 (d, 1H, J = 5.2 Hz, C6″*H*), 8.45 (s,1H, C3′*H*), 8.44 (s, 1H, C5′*H*), 8.37 (t, 2H, J = 6.5 Hz, C3*H*/C3″*H*), 8.01 (t, 2H, J = 7.6 Hz, C4*H*/C4″*H*), 7.71 (t, 2H, J = 6.1 Hz, C5*H*/C5″*H*), 6.05 (d, 1H, J = 7.7 Hz, N*H* dach), 5.19 (m, 1H, N*H* dach), 2.76−2.61 (m, 2H, N*H* + C*H* dach), 2.61−2.51 (m, 1H, C*H* dach), 2.37 (m, 1H, N*H* dach), 2.09−1.97 (m, 1H, C*H* dach), 1.83−1.69 (m, 2H, C*H* dach), 1.55 (d, 2H, J = 10.1 Hz, C*H* dach), 1.24 (m, 1H, C*H* dach), 1.11 (m, 1H, C*H* dach), 0.89 (m, 1H, C*H* dach). ^{1}H NMR (CD_3NO_2): δ 8.98 (d, 1H, J = 5.4 Hz, C6*H*), 8.93 (d, 1H, J = 5.1 Hz, C6″*H*), 8.42 (t, 2H, J = 8.9 Hz, C3*H*/C3″*H*), 8.37 (dd, 2H, J = 10.7 and 1.7 Hz, C3′*H*/C5′*H*), 8.05 (t, 2H, J = 7.8 Hz, C4*H*/C4″*H*), 7.72 (m br, 2H, C5*H*/C5″*H*), 5.68 (d br, 1H, N*H* dach), 4.85 (t, 1H, J = 12.2 Hz, N*H* dach), 2.94 (m, 1H, C*H* dach), 2.69 (d br, 1H, CH_2 dach), 2.31 (m, 1H, C*H* dach), 2.11 (overlapped with the H_2O resonance, N*H* dach), 1.92−1.79 (m, 2H, CH_2 dach), 1.74 (br m, 1H, N*H* dach), 1.68 (d br, 1H, J = 13.1 Hz, CH_2 dach), 1.59 (d br, 1H, J = 12.7 Hz, CH_2 dach), 1.34 (m, 1H, CH_2 dach), 1.21 (m, 1H, CH_2 dach), 1.01 (ddd, 2H, J = 24.9, 12.5, and 3.5 Hz, CH_2 dach). ^{13}C NMR (CD_3NO_2): δ 162.44 (*C*2′), 162.37 (*C*6′), 160.8 (*C*2), 160.7 (*C*2″), 153.7 (6″H), 153.6 (*C*6H), 137.6 (*C*4H), 137.5 (*C*4″H), 137.0 (*C*4′), 128.9 (*C*5″H), 128.6 (*C*5H), 124.4 (*C*3H), 124.3 (*C*3″H), 122.54 (*C*3′H), 122.48 (*C*5′H), 61.9 (*C*H dach), 61.7 (*C*H dach), 36.4 (*C*H_2 dach), 35.1 (*C*H_2 dach), 25.7 (*C*H_2 dach), 25.3 (*C*H_2 dach). Selected IR (KBr, cm^{-1}): ν_{NH} 3285 (m); ν_{tpy} 2930 (m), 1602 (s), 1472 (m), 1423 (m), 1109 (s), 785 (s), 563 (w); ν_{Ru-Cl} 310 (w). UV/visible spectrum [H_2O; λ_{max}, nm (ε, M^{-1} cm^{-1})]: 239 (24530), 278 (21080), 317 (29220), 369 (4430), 502 (4690), 561 (4010).

[Ru(Cl-tpy)(bpy)Cl][Cl] (***3*$_{Cl}$**). A total of 50.0 mg (0.105 mmol) of **P1**, 19.7 mg (0.126 mmol) of bpy, 44.5 mg (1.050 mmol) of LiCl, and 43.9 μL (0.315 mmol) of Et_3N in 10 mL of ethanol/water afforded **3** as a dark-red crystalline solid. Yield: 48.8 mg (78%). An alternative, less efficient, preparation of this complex has been recently reported.[25] Anal. Calcd for $C_{25}H_{18}Cl_3N_5Ru$ (595.87): C, 50.4; H, 3.04; N, 11.75. Found: C, 50.4; H, 3.13; N, 11.71. Crystals suitable for X-ray analysis were obtained from an aqueous solution of $\mathbf{3}_{Cl}$ to which an excess of NaCl had been added. Complex **3** is soluble in water, methanol, ethanol, acetone, chloroform, dichloromethane, and nitromethane. ^{1}H NMR (D_2O): δ 9.95 (d, 1H, J = 5.5 Hz, Ca*H*), 8.67 (s, 2H, C3′*H*/C5′*H*), 8.66 (d, 1H, J = 8.4 Hz, Cd*H*), 8.41 (d, 2H, J = 8.0 Hz, C3*H*/C3″*H*), 8.36−8.29 (m, 2H, Cg*H*/*Cc*H), 7.99 (t, 1H, J = 6.4 Hz, Cb*H*), 7.93 (t, 2H, J = 7.8 Hz, C4*H*/C4″*H*), 7.79 (d, 2H, J = 5.3 Hz, C6*H*/C6″*H*), 7.70 (t, 1H, J = 7.9 Hz, Ch*H*), 7.38−7.29 (m, 3H, Cj*H*/C5*H*/C5″*H*), 6.95 (t, 1H, J = 6.7 Hz, Ci*H*). ^{13}C NMR (D_2O): δ 158.9 (*C*2′/*C*6′), 158.6 (Cf), 157.6 (*C*2/*C*2″), 156.1 (Ce), 152.5 (*C*6H/*C*6″H), 151.8 (CjH), 151.8 (CaH), 141.8 (*C*4′), 137.5 (*C*4H/*C*4″H), 137.0 (CcH), 135.9 (ChH), 127.7 (*C*5H/*C*5″H), 126.9 (CbH), 125.8 (CiH), 124.1 (*C*3H/*C*3″H), 123.4 (CdH), 123.1 (CgH), 123.0 (*C*3′H/*C*5′H). Selected IR (KBr, cm^{-1}): ν_{tpy} 3043 (m), 1600 (m), 1463 (m), 1421 (s), 1117 (s), 788 (s), 568 (m); ν_{Ru-Cl} 351 (w). UV/visible spectrum [H_2O; λ_{max}, nm (ε, M^{-1} cm^{-1})]: 239 (19670), 281 (19500), 290 (19240), 313 (18090), 488 (5810).

[Ru(tpy)(en)Cl][Cl] (***4*$_{Cl}$**). A total of 100.0 mg (0.227 mmol) of **P2**, 18.2 μL (0.272 mmol) of en, 96.0 mg (2.264 mmol) of LiCl, and 94.7 μL (0.679 mmol) of Et_3N in 22 mL of ethanol/water afforded **4** as a dark-purple solid. Yield: 46.4 mg (44%). Anal. Calcd for $C_{17}H_{19}Cl_2N_5Ru$ (465.34): C, 43.9; H, 4.12; N, 15.05. Found: C, 44.0; H, 4.18; N, 15.00. The synthesis of this complex has been reported previously, as an intermediate in the preparation of the aqua species $[Ru(tpy)(en)(H_2O)][ClO_4]_2$, with insufficient characterization.[26] Here, we described a slightly modified preparation, with unambiguous characterization of the product. Complex **4** is soluble in water, methanol, and ethanol and slightly soluble in acetone and nitromethane, whereas it is insoluble in chloroform and dichloromethane. ^{1}H NMR (D_2O): δ 8.92 (d, 2H, J = 5.5 Hz, C6*H*/C6″*H*), 8.40 (d, 2H, J = 7.9 Hz, C3*H*/C3″*H*), 8.36 (d, 2H, J = 8.1 Hz, C3′*H*/C5′*H*), 8.00 (t, 2H, J = 7.2 Hz, C4*H*/C4″*H*), 7.82 (t, 1H, J = 8.0 Hz, C4′*H*), 7.68 (m, 2H, C5*H*/C5″*H*), 5.62 (t br, 2H, NH_2 en), 3.24 (m br, 2H, CH_2 en), 2.62 (t br, 2H, NH_2 en), 2.34 (m br, 2H, CH_2 en). ^{1}H NMR (CD_3NO_2): δ 8.96 (d, 2H, J = 5.8 Hz, C6*H*/C6″*H*), 8.41 (d, 2H, J = 7.6 Hz, C3*H*/C3″*H*), 8.36 (d, 2H, J = 8.0 Hz, C3′*H*/C5′*H*), 8.02 (td, 2H, J = 7.8 and 1.5 Hz, C4*H*/C4″*H*), 7.81 (t, 1H, J = 8.0 Hz, C4′*H*), 7.69 (m, 2H, C5*H*/C5″*H*), 5.33 (s br, 2H, NH_2 en), 3.46 (m, 2H, CH_2 en), 2.61 (m, 2H, CH_2 en), 2.03 (s br, 2H, NH_2 en). ^{13}C NMR (CD_3NO_2): δ 161.8 (*C*2′/*C*6′), 161.6 (*C*2/*C*2″), 153.5 (*C*6H/*C*6″H), 137.4 (*C*4H/*C*4″H), 130.7 (*C*4′H), 128.2 (*C*5H/*C*5″H), 123.8 (*C*3H/*C*3″H), 122.4 (*C*3′H/*C*5′H), 46.9 (*C*H_2 en), 46.8 (*C*H_2 en). Selected IR (KBr, cm^{-1}): ν_{NH} 3233 (m), 3152 (m); ν_{tpy} 3055 (m), 2937 (m), 1616 (m), 1447 (s), 1116 (s), 767 (s), 619 (m); ν_{Ru-Cl} 309 (w). UV/visible spectrum [λ_{max}, nm (ε, M^{-1} cm^{-1})]: 232 (20830), 274 (20151), 317 (28290), 368 (3800), 481 (4433), 539 (3524).

[Ru(tpy)(dach)Cl][Cl] (***5*$_{Cl}$**). A total of 50.0 mg (0.113 mmol) of **P2**, 16.3 μL (0.136 mmol) of dach, 47.9 mg (1.130 mmol) of LiCl, and 47.0 μL (0.339 mmol) of Et_3N in 10 mL of ethanol/water (3:1) afforded **5** as a dark-purple solid. Yield: 41.2 mg (70%). Anal. Calcd for $C_{21}H_{25}Cl_2N_5Ru$ (519.43): C, 48.6; H, 4.85; N, 13.48. Found: C, 48.8; H, 4.79; N, 13.52. Complex **5** is soluble in water, methanol, and ethanol and partially soluble in nitromethane, whereas it is insoluble in acetone, chloroform, and dichloromethane. ^{1}H NMR (D_2O): δ 8.97 (d, 1H, J = 5.3 Hz, C6*H*), 8.88 (d, 1H, J = 5.6 Hz, C6″*H*), 8.40 (t, 2H, C3*H*/C3″*H*), 8.36 (t, 2H, J = 8.1 Hz, C3′*H*/C5′*H*), 8.00 (m, 2H, C4*H*/C4″*H*), 7.81 (t, 1H, J = 8.1 Hz, C4′*H*), 7.68 (m, 2H, C5*H*/C5″*H*), 5.97 (dd, 1H, J = 11.9 and 4.7 Hz, N*H* dach), 5.11 (t, 1H, J = 11.3 Hz, N*H* dach), 2.76−2.52 (m, 3H, N*H* + C*H* + CH_2 dach), 2.34 (t, 1H, J = 10.7 Hz, N*H* dach), 2.10−1.96 (m, 1H, CH_2 dach), 1.83−1.68 (m, 2H, CH_2 dach), 1.55 (d, 2H, J = 11.9 Hz, CH_2 dach), 1.24 (m, 1H, CH_2 dach), 1.11 (m, 1H, CH_2 dach), 0.88 (m, 1H, CH_2 dach). ^{1}H NMR (CD_3NO_2): δ 8.98 (d, 1H, J = 5.1 Hz, C6*H*), 8.92 (d, 1H, J = 5.0 Hz, C6″*H*), 8.41 (t, 2H, J = 9.3 Hz, C3*H*/C3″*H*), 8.36 (dd, 2H, J = 9.5 and 8.4 Hz, C3′*H*/C5′*H*), 8.01 (t, 2H, J = 7.8 Hz, C4*H*/C4″*H*), 7.80 (t, 1H, J = 8.0 Hz, C4′*H*), 7.67 (m br, 2H, C5*H*/C5″*H*), 5.64 (d br, 1H, N*H* dach), 4.81 (t, 1H, J = 12.2 Hz, N*H* dach), 2.92 (m, 1H, C*H* dach), 2.68 (m, 1H, CH_2 dach), 2.31 (m, 1H, C*H* dach), 2.00 (partially overlapped with the H_2O resonance, N*H* dach), 1.87−1.79 (m, 3H, 2 × CH_2 + N*H* dach), 1.68 (d br, 1H, J = 12.7 Hz, CH_2 dach), 1.59 (d br, 1H, J = 12.2 Hz, CH_2 dach), 1.34 (m, 1H, CH_2 dach), 1.21 (m, 1H, CH_2 dach), 1.01 (ddd, 1H, J = 25.4, 12.6, and 3.7 Hz, CH_2 dach). ^{13}C NMR (CD_3NO_2): δ 161.78 (*C*2), 161.75 (*C*2″), 161.66 (*C*2′), 161.57 (*C*6′), 153.6 (*C*6H/6″H), 137.4 (*C*4H), 137.3 (*C*4″H), 130.6 (*C*4′H), 128.3 (*C*5H), 128.1 (*C*5″H), 123.8 (*C*3H), 123.7 (*C*3″H), 122.44 (*C*3′H), 122.36 (*C*5′H), 61.8 (*C*H dach), 61.7 (*C*H dach), 36.5 (*C*H_2 dach), 35.2 (*C*H_2 dach), 25.7 (*C*H_2 dach), 25.3 (*C*H_2 dach). Selected IR (KBr, cm^{-1}): ν_{NH} 3240 (m), 3141 (m); ν_{tpy} 2931 (s), 2856 (m), 1601 (s), 1446 (s), 1112 (m), 768 (s), 618 (m); ν_{Ru-Cl} 310 (w). UV/visible spectrum [λ_{max}, nm (ε, M^{-1} cm^{-1})]: 233 (23896), 274 (23385), 318 (33757), 370 (4354), 493 (4660), 544 (4194).

General Synthetic Procedure for [Ru(Cl-tpy)(N-N)(dmso-*S*)][CF_3SO_3]$_2$ ($\mathbf{6}_{OTf}$**−**$\mathbf{8}_{OTf}$**) and [Ru(tpy)(N-N)(dmso-*S*)][CF_3SO_3]$_2$ (**$\mathbf{9}_{OTf}$ **and** $\mathbf{10}_{OTf}$**).** A weighed amount of [Ru(Cl-tpy)(N-N)Cl][Cl] [N-N = en ($\mathbf{1}_{Cl}$), dach ($\mathbf{2}_{Cl}$), and bpy ($\mathbf{3}_{Cl}$)] was dissolved in a solution of methanol containing a great excess (ca. 35 equiv) of DMSO. After the addition of 2.1 equiv of $AgCF_3SO_3$, the reaction mixture was heated to reflux for 2 h in the dark. During this time, the color of the solution changed from violet (dark red for $\mathbf{8}_{OTf}$) to red-orange. At the end, AgCl was removed by filtration over Celite, and methanol was evaporated under reduced pressure. The oily residue was dissolved with ethanol, diethyl ether was added dropwise until saturation, and the solution was stored at 4 °C for 24−48 h, which induced formation of the corresponding product as a red-orange crystalline solid. The solid was collected by filtration, washed with cold ethanol/diethyl ether and diethyl ether, and vacuum-dried.

The corresponding tpy complexes $\mathbf{9}_{OTf}$ and $\mathbf{10}_{OTf}$ were prepared with a similar procedure using $\mathbf{4}_{Cl}$ and $\mathbf{5}_{Cl}$, respectively, as starting materials.

[Ru(Cl-tpy)(en)(dmso-S)][CF_3SO_3]$_2$ (***6*$_{OTf}$**). A total of 25.0 mg (0.050 mmol) of $\mathbf{1}_{Cl}$ and 27.0 mg (0.105 mmol) of $AgCF_3SO_3$ in a solution of 7 mL of methanol containing 125.0 μL of DMSO afforded $\mathbf{6}_{OTf}$ as red-

dx.doi.org/10.1021/ic5005215 | *Inorg. Chem.* 2014, 53, 6113−6126

orange needles suitable for X-ray analysis. Yield: 33.4 mg (83%). Anal. Calcd for $C_{21}H_{24}ClF_6N_5O_7RuS_3$ (805.15): C, 31.3; H, 3.00; N, 8.70. Found: C, 31.3; H, 3.03; N, 8.67. Complex $\mathbf{6}_{OTf}$ is soluble in water, methanol, ethanol, acetone, and acetonitrile, whereas it is insoluble in chloroform and dichloromethane. ^{1}H NMR ($(CD_3)_2CO$): δ 9.23 (d, 2H, J = 5.5 Hz, C6*H*/C6″*H*), 8.86 (s, 2H, C3′*H*/C5′*H*), 8.81 (d, 2H, J = 7.6 Hz, C3*H*/C3″*H*), 8.39 (t, 2H, J = 7.8 Hz, C4*H*/C4″*H*), 7.95 (t, 2H, C5*H*/C5″*H*), 5.62 (t br, 2H, NH_2 en), 4.18 (t br, 2H, NH_2 en), 3.37 (m br, 2H, CH_2 en), 2.95 (m br, 2H, CH_2 en), 2.52 (s, 6H, CH_3 dmso-*S*). ^{13}C NMR ($(CD_3)_2CO$): δ 160.2 (*C*2′/*C*6′), 159.5 (*C*2/*C*2″), 154.9 (*C*6H/*C*6″H), 144.4 (*C*4′), 140.1 (*C*4H/*C*4″H), 129.8 (*C*5H/*C*5″H), 126.1 (*C*3H/*C*3″H), 124.5 (*C*3′H/*C*5′H), 46.6 (*C*H_2 en), 45.7 (*C*H_2 en), 43.3 (*C*H_3 dmso-*S*). Selected IR (KBr, cm^{-1}): ν_{NH} 3274 (m), 3191 (m), 3169 (m); ν_{tpy} 3070 (m), 1598 (s), 1473 (m), 1425 (s), 1125 (s), 794 (s); $\nu_{S=O}$ 1087 (s); ν_{OTf} 1246 (vs), 1222 (vs), 1163 (vs), 1025 (vs); ν_{Ru-S} 423 (s). UV/visible spectrum [H_2O; λ_{max}, nm (ε, M^{-1} cm^{-1})]: 236 (45432), 273 (40473), 289 (45396), 329 (32826), 420 (8220).

[Ru(Cl-tpy)(dach)(dmso-S)][CF$_3$SO$_3$]$_2$ ($\mathbf{7}_{OTf}$). A total of 25.0 mg (0.045 mmol) of $\mathbf{2}_{Cl}$ and 24.3 mg (0.095 mmol) of $AgCF_3SO_3$ in a solution of 6 mL of methanol containing 113.0 μL of DMSO afforded $\mathbf{7}_{OTf}$ as red-orange plates. Yield: 34.5 mg (89%). Anal. Calcd for $C_{25}H_{30}ClF_6N_5O_7RuS_3$ (859.24): C, 35.0; H, 3.52; N, 8.15. Found: C, 34.9; H, 3.59; N, 8.09. Complex $\mathbf{7}_{OTf}$ is soluble in water, methanol, ethanol, acetone, and acetonitrile, whereas it is insoluble in chloroform and dichloromethane. ^{1}H NMR ($(CD_3)_2CO$): δ 9.32 (d, 1H, J = 5.4 Hz, C6*H*), 9.17 (d, 1H, J = 5.4 Hz, C6″*H*), 8.84 (s, 1H, C3′*H*), 8.83 (s, 1H, C5′*H*), 8.79 (dd, 2H, J = 7.9 and 4.6 Hz, C3*H*/C3″*H*), 8.37 (dd, 2H, J = 13.9 and 6.5 Hz, C4*H*/C4″*H*), 7.93 (dd, 2H, J = 12.6 and 6.3 Hz, C5*H*/C5″*H*), 5.79 (d br, 1H, J = 9.5 Hz, N*H* dach), 5.09 (t br, 1H, J = 11.9 Hz, N*H* dach), 4.27 (d br, 1H, J = 10.0 Hz, N*H* dach), 3.94 (t, 1H, J = 11.6 Hz, N*H* dach), 2.95 (m, 1H, C*H* dach), 2.65 (m, 1H, C*H* dach), 2.56 (d br, 1H, J = 13.4 Hz, CH_2 dach), 2.52 (s, 3H, CH_3 dmso-*S*), 2.46 (s, 3H, CH_3 dmso-*S*), 1.83 (m br, 2H, CH_2 dach), 1.78 (d br, 1H, J = 15.3 Hz, CH_2 dach), 1.61 (d br, 1H, J = 12.2 Hz, CH_2 dach), 1.35−1.15 (m, 3H, CH_2 dach). ^{13}C NMR ($(CD_3)_2CO$): δ 160.4 (*C*2′), 160.1 (*C*6′), 159.7 (*C*2), 159.4 (*C*2″), 155.2 (*C*6″H), 155.0 (*C*6H), 144.3 (*C*4′), 140.1 (*C*4H), 140.1 (*C*4″H), 129.9 (*C*5″H), 129.8 (*C*5H), 126.10 (*C*3H), 126.09 (*C*3″H), 124.5 (*C*3′H), 124.4 (*C*5′H), 61.4 (*C*H dach), 60.3 (*C*H dach), 43.6 (*C*H_3 dmso-*S*), 43.0 (*C*H_3 dmso-*S*), 35.1 (*C*H_2 dach), 34.8 (*C*H_2 dach), 25.2 (*C*H_2 dach), 24.8 (*C*H_2 dach). Selected IR (KBr, cm^{-1}): ν_{NH} 3263 (m), 3186 (m), 3169 (m); ν_{tpy} 3059 (m), 2932 (m), 1595 (s), 1472 (w), 1426 (m), 1122 (s), 786 (s), 574 (m); $\nu_{S=O}$ 1085 (s); ν_{OTf} 1253 (vs), 1224 (vs), 1160 (vs), 1028 (vs); ν_{Ru-S} 419 (s). UV/visible spectrum [H_2O; λ_{max}, nm (ε, M^{-1} cm^{-1})]: 236 (40275), 273 (34830), 294 (39110), 329 (28820), 421 (8027).

[Ru(Cl-tpy)(bpy)(dmso-S)][CF$_3$SO$_3$]$_2$ ($\mathbf{8}_{OTf}$). A total of 25.0 mg (0.042 mmol) of $\mathbf{3}_{Cl}$ and 22.6 mg (0.088 mmol) of $AgCF_3SO_3$ in a solution of 6 mL of methanol containing 105.0 μL of DMSO afforded $\mathbf{8}_{OTf}$ as red-orange plates suitable for X-ray analysis. Yield: 32.9 mg (87%). Anal. Calcd for $C_{29}H_{24}ClF_6N_5O_7RuS_3$ (901.24): C, 38.7; H, 2.68; N, 7.77. Found: C, 38.7; H, 2.69; N, 7.79. Complex $\mathbf{8}_{OTf}$ is soluble in water, methanol, ethanol, acetone, and acetonitrile, whereas it is insoluble in chloroform and dichloromethane. ^{1}H NMR [$(CD_3)_2CO$]: δ 10.31 (d, 1H, J = 5.6 Hz, Ca*H*), 9.12 (s, 2H, C3′*H*/C5′*H*), 8.95 (d, 1H, J = 8.0 Hz, Cd*H*), 8.88 (d, 2H, J = 8.0 Hz, C3*H*/C3″*H*), 8.75 (d, 1H, J = 8.0 Hz, Cg*H*), 8.51 (td, 1H, J = 7.9 and 1.4 Hz, Cc*H*), 8.30 (td, 2H, J = 7.9 and 1.4 Hz, C4*H*/C4″*H*), 8.17 (d, 2H, J = 5.4 Hz, C6*H*/C6″*H*), 8.15 (t, 1H J = 8.1 Hz, Cb*H*), 8.11 (td, 1H, J = 8.1 and 1.4 Hz, Ch*H*), 7.66 (ddd, 2H, J = 7.5, 5.5, and 1.2 Hz, C5*H*/C5″*H*), 7.60 (d, 1H, J = 5.6 Hz, Cj*H*), 7.38 (t, 1H, J = 6.7 Hz, Ci*H*), 2.67 (s, 6H, CH_3 dmso-*S*). ^{13}C NMR [$(CD_3)_2CO$]: δ 159.3 (*C*2′/*C*6′), 157.8 (*C*2/*C*2″), 157.5 (*C*e), 156.9 (*C*f), 156.0 (*C*aH), 155.2 (*C*6H/*C*6″H), 150.2 (*C*jH), 147.2 (*C*4′), 140.7 (*C*4H/*C*4″H), 140.4 (*C*hH), 139.9 (*C*cH), 130.5 (*C*5H/*C*5″H), 128.9 (*C*bH), 128.6 (*C*iH), 127.1 (*C*3H/*C*3″H), 126.6 (*C*3′H/*C*5′H), 125.7 (*C*dH), 124.9 (*C*gH), 42.9 (*C*H_3 dmso-*S*). Selected IR (KBr, cm^{-1}): ν_{tpy} 3073 (m), 3012 (m), 2923 (m), 1598 (s), 1472 (w), 1424 (m), 1123 (s), 791 (m), 570 (m); $\nu_{S=O}$ 1093 (s); ν_{OTf} 1260 (vs), 1222 (s), 1145 (s), 1028 (vs); ν_{Ru-S} 430 (s). UV/visible spectrum [H_2O; λ_{max}, nm (ε, M^{-1} cm^{-1})]: 236 (30530), 249 (27538) 274 (41680), 284 (39942), 314 (23230), 329 (26052), 405 (7996), 520 (428).

[Ru(tpy)(en)(dmso-S)][CF$_3$SO$_3$]$_2$ ($\mathbf{9}_{OTf}$). A total of 25.0 mg (0.054 mmol) of $\mathbf{4}_{Cl}$ and 29.0 mg (0.113 mmol) of $AgCF_3SO_3$ in a solution of 6.5 mL of methanol containing 125.0 μL of DMSO afforded $\mathbf{9}_{OTf}$ as red-orange needles. Yield: 36.1 mg (87%). Anal. Calcd for $C_{21}H_{25}F_6N_5O_7RuS_3$ (770.71): C, 32.7; H, 3.27; N, 9.09. Found: C, 32.6; H, 3.23; N, 9.11. Complex $\mathbf{9}_{OTf}$ is soluble in water, methanol, ethanol, acetone, and acetonitrile, whereas it is insoluble in chloroform and dichloromethane. ^{1}H NMR [$(CD_3)_2CO$]: δ9.22 (d, 2H, J = 5.1 Hz, C6*H*/C6″*H*), 8.72 (d, 2H, J = 7.8 Hz, C3*H*/C3″*H*), 8.71 (d, 2H, J = 8.1 Hz, C3′*H*/C5′*H*), 8.34 (td, 2H, J = 8.0 and 1.5 Hz, C4*H*/C4″*H*), 8.32 (t, 1H, J = 8.1 Hz, C4′*H*), 7.90 (ddd, 2H, J = 7.4, 5.6, and 1.2 Hz, C5*H*/C5″*H*), 5.61 (m br, 2H, NH_2 en), 4.20 (m br, 2H, NH_2 en), 3.36 (dt, 2H, J = 11.4 and 5.8 Hz, CH_2 en), 2.94 (dt, 2H, J = 11.0 and 5.6 Hz, CH_2 en), 2.52 (s, 6H, CH_3 dmso-*S*). ^{13}C NMR [$(CD_3)_2CO$]: δ 160.4 (*C*2/*C*2″), 159.2 (*C*2′/*C*6′), 154.9 (*C*6H/*C*6″H), 140.0 (*C*4H/*C*4″H), 137.4 (*C*4′H), 129.3 (*C*5H/*C*5″H), 125.5 (*C*3H/*C*3″H), 124.2 (*C*3′H/*C*5′H), 46.6 (*C*H_2 en), 45.7 (*C*H_2 en), 43.5 (*C*H_3 dmso-*S*). Selected IR (KBr, cm^{-1}): ν_{NH} 3243 (m), 3165 (m); ν_{tpy} 3077 (m), 1603 (m), 1449 (m), 778 (s), 573 (s); $\nu_{S=O}$ 1071 (m); ν_{OTf} 1246 (vs), 1222 (vs), 1155 (vs), 1024 (vs); ν_{Ru-S} 426 (s). UV/visible spectrum [H_2O; λ_{max}, nm (ε, M^{-1} cm^{-1})]: 239 (33153), 272 (40851), 287 (46104), 330 (35481), 421 (8139).

[Ru(tpy)(dach)(dmso-S)][CF$_3$SO$_3$]$_2$ ($\mathbf{10}_{OTf}$). A total of 25.0 mg (0.048 mmol) of $\mathbf{5}_{Cl}$ and 26.0 mg (0.101 mmol) of $AgCF_3SO_3$ in a solution of 6 mL of methanol containing 120.0 μL of DMSO afforded $\mathbf{10}_{OTf}$ as red-orange plates. Yield: 32.4 mg (82%). Anal. Calcd for $C_{25}H_{31}F_6N_5O_7RuS_3$ (824.80): C, 36.4; H, 3.79; N, 8.49. Found: C, 36.3; H, 3.86; N, 8.52. Complex $\mathbf{10}_{OTf}$ is soluble in water, methanol, ethanol, acetone, and acetonitrile, whereas it is insoluble in chloroform and dichloromethane. ^{1}H NMR [$(CD_3)_2CO$]: δ 9.34 (d, 1H, J = 5.0 Hz, C6*H*), 9.20 (d, 1H, J = 5.0 Hz, C6″*H*), 8.74−8.61 (m, 4H, C3*H*/C3″*H*/C3′*H*/C5′*H*), 8.36−8.20 (m, 3H, C4*H*/C4″*H*/C4′*H*), 7.92−7.75 (m, 2H, C5*H*/C5″*H*), 5.85 (d, 1H, J = 10.8 Hz, N*H* dach), 5.04 (t, 1H, J = 11.2 Hz, N*H* dach), 4.35 (d, 1H, J = 10.7 Hz, N*H* dach), 3.93 (t, 1H, J = 11.6 Hz, N*H* dach), 2.90−2.82 (m, 1H, C*H* dach), 2.62−2.47 (m, 8H, C*H* dach + 2 × CH_3 dmso-*S* + CH_2 dach), 1.89−1.70 (m, 3H, 3 × CH_2 dach), 1.60 (d, 1H, J = 9.6 Hz, CH_2 dach), 1.38−1.15 (m, 3H, 3 × CH_2 dach). ^{13}C NMR ($(CD_3)_2CO$): δ 160.0 (*C*2′), 159.9 (*C*2), 159.7 (*C*6′), 159.6 (*C*2″), 155.5 (*C*6″H), 155.1 (*C*6H), 139.8 (*C*4H/*C*4″H), 137.3 (*C*4′H), 129.3 (*C*5″H), 129.1 (*C*5H), 125.41 (*C*3H), 125.36 (*C*3″H), 124.1 (*C*3′H), 124.0 (*C*5′H), 61.6 (*C*H dach), 60.1 (*C*H dach), 44.0 (*C*H_3 dmso-*S*), 43.9 (*C*H_3 dmso-*S*), 35.1 (*C*H_2 dach), 34.7 (*C*H_2 dach), 25.3 (*C*H_2 dach), 24.9 (*C*H_2 dach). Selected IR (KBr, cm^{-1}): ν_{NH} 3282 (m), 3240 (m), 3157 (m); ν_{tpy} 2936 (m), 2878 (m), 1603 (m), 1445 (s), 774 (s), 572 (m); $\nu_{S=O}$ 1100 (s); ν_{OTf} 1251 (vs), 1220 (vs), 1161 (vs), 1022 (vs); ν_{Ru-S} 429 (s). UV/visible spectrum [H_2O; λ_{max}, nm (ε, M^{-1} cm^{-1})]: 239 (36975), 272 (43410), 296 (51957), 330 (38535), 418 (8337).

X-ray Crystallography. X-ray diffraction data for compounds $\mathbf{6}_{OTf}$ and $\mathbf{8}_{OTf}$ were collected at 150(2) K on an Oxford Diffraction SuperNova diffractometer equipped with mirror optics and an Atlas detector by using Mo and Cu microfocus X-ray sources, respectively. Intensity data for $\mathbf{3}_{Cl}$ and $\mathbf{6}_{PF_6}$ were carried out at the X-ray diffraction beamline of synchrotron Elettra (Trieste) at 100 K, with λ = 0.7000 and 0.88560 Å, respectively. Cell refinement, indexing, and scaling of the data sets were carried out using *CrysAlis Pro*, *Mosflm*, and *Scala*.[27] The structures were solved by direct methods implemented in *SIR92*[28] and refined by a full-matrix least-squares procedure based on F^2 using *SHELXL-97*.[29] All non-hydrogen atoms were refined anisotropically. The hydrogen atoms were placed at calculated positions and treated using the appropriate riding models. The programs *Mercury*, *ORTEP*, *Platon*, and *Diamond Crystal* were used for data analysis and figure preparation.[30] Crystal data and details of refinement are given in Table S1 in the SI.

Interactions with Nucleobases. (a) 9MeG: NMR samples of complexes **1**−**3** (4 mM) were prepared in D_2O. When hydrolysis of

dx.doi.org/10.1021/ic5005215 | *Inorg. Chem.* 2014, 53, 6113−6126

Scheme 1. Synthetic Pathways for the Preparation of Complexes 1−10[a]

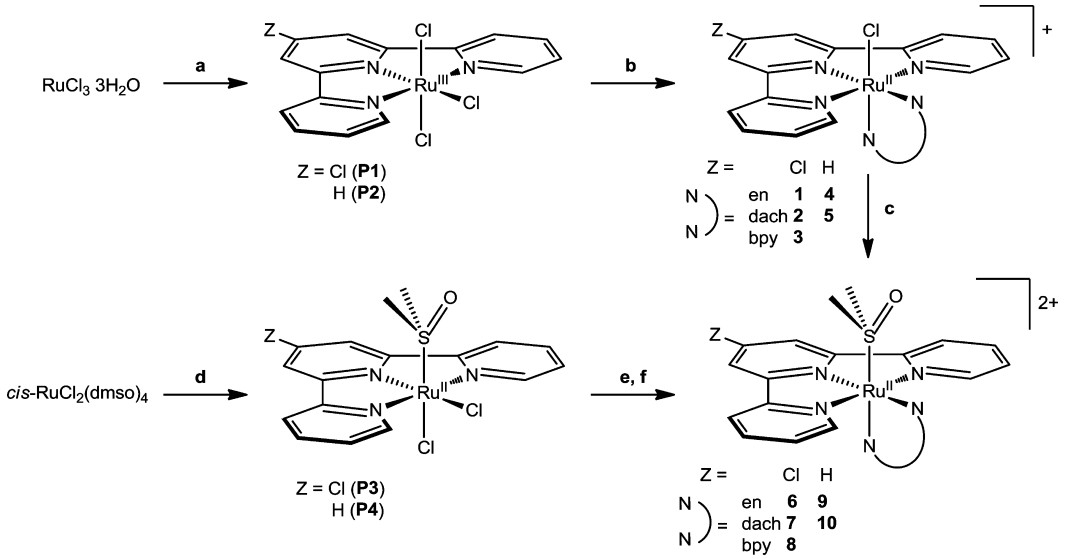

[a]Reagents and conditions: (a) Cl-tpy or tpy (0.9 equiv), EtOH, reflux; (b) N-N (1.2 equiv; N-N = en, dach, or bpy), ethanol/water (3:1), Et_3N (3.0 equiv), LiCl (10.0 equiv), reflux; (c) DMSO (35 equiv), $AgCF_3SO_3$ (2.1 equiv), MeOH, reflux; (d) Cl-tpy or tpy (1.1 equiv), CH_3Cl; (e) N-N (1.2 equiv; N-N = en, dach, or bpy), $CHCl_3$/EtOH (2:3), reflux; (f) excess NH_4PF_6.

the complex was completed, 1 equiv of solid 9MeG was added. (b) 5′-GMP: NMR samples of complexes **1**−**3** (10 mM) were prepared in D_2O. When hydrolysis of the complex was completed, 1 equiv of solid 5′-GMP was added. (c) 5′-AMP: The pH of a solution of 5′-AMP in D_2O (0.4 mL, 12.5 mM) was adjusted to ca. 7.00, and then a solution of **1aq** in D_2O (0.1 mL, 50.0 mM) was added. (d) 5′-AMP/5′-GMP competition: an NMR sample containing a 1:1 mixture of 5′-AMP and 5′-GMP in D_2O (0.4 mL, 12.5 mM) was prepared and the pH adjusted to ca. 7.00. To this sample was added a solution of **1aq** in D_2O (0.1 mL, 50.0 mM).

pH Titrations. (a) Aqua species **1aq**−**3aq**: NMR samples of complexes **1**−**3** were prepared in a concentration of 4 mM in 10% D_2O/90% H_2O 24 h prior to titrations in order to ensure complete hydrolysis of the complexes. (b) Guanine adducts **11** and **12**: The NMR samples used to monitor formation of these adducts in D_2O [i.e., **1** + 9MeG (4 mM, 1:1.3) for **11** and **1** + 5′-GMP (10 mM, 1:1) for **12**] were used for the titrations, performed 6 days after the mixing.

The pH values of the NMR samples were measured at 298 K directly in the NMR tube using an AMEL (model 334B) pH meter equipped with an Ingold microcombination electrode calibrated with Ingold buffer solutions at pH = 4.0, 7.0, and 10.0. The pH values were adjusted with diluted $DClO_4$ and NaOD solutions. No correction was applied for the effect of deuterium on the glass electrode.

Calculation of pK_a Values. The pH titration curves were fitted to the Henderson−Hasselbalch equation using the program *Origin 8* with the assumption that the observed chemical shifts are weighted averages according to the populations of the protonated and deprotonated species.

Kinetic Analysis. The hydrolysis kinetics of complexes **1** and **2** were studied by UV/visible spectroscopy at 298 K. The samples (0.10 mM) were prepared in distilled water or in a buffer solution (25 mM Hepes buffer, pH = 7.4). The working wavelength of each reaction corresponded to that of a maximum change in absorption derived from the difference spectra. The absorbance at the selected wavelength was recorded at 30 s intervals, and the absorption/time data for each complex were computer-fitted to the first-order rate equation (eq 1), which gave the k_{H_2O} value (k) for each aquation process:

$$A = C_0 + C_1 e^{-kt} \quad (1)$$

C_0 and C_1 are computer-fitted constants, and A is the absorbance at time t.

The kinetics of the substitution reactions of complexes **1** and **2** with guanine derivatives (9MeG and 5′-GMP) were also studied spectrophotometrically. All kinetic measurements were performed under pseudo-first-order conditions (i.e., the concentration of the nucleophile was at least 10-fold that of the complex). The reactions were initiated by mixing a solution of each complex (0.3 mL, 1.00 mM) with 2.7 mL of a thermally equilibrated nucleophile solution (5.56 mM) in the UV/visible cuvette, and the reactions were followed for at least 8 half-lives. The observed pseudo-first-order rate constants, k_{obsd}, represent an average value of two to three independent kinetic runs for each experimental condition. Reactions were studied at three different temperatures (298, 310, and 318 K) in 25 mM Hepes buffer containing 30 mM NaCl at pH = 7.40. The second-order rate constants k_2 for the substitution reactions with guanine derivatives were obtained directly from the slopes of k_{obsd} plots versus the concentration of the nucleophile. All kinetic data were computer-fitted to the appropriate equation using the programs *Microsoft Excel 2007* and *Origin 8*.

RESULTS AND DISCUSSION

Synthesis and Characterization of the Complexes. Treatment of the neutral ruthenium(III) precursors *mer*-[Ru(L_3)Cl_3] [L_3 = Cl-tpy (**P1**) or tpy (**P2**)] with a neutral N-N chelating ligand, such as en, dach, or bpy, in the presence of Et_3N as the reductant and an excess of LiCl, needed to prevent Cl^- dissociation from the final products and necessary for their precipitation, afforded the cationic ruthenium(II) complexes [Ru(Cl-tpy)(N-N)Cl][Cl] [N-N = en (**1**), dach (**2**), and bpy (**3**)] and [Ru(tpy)(N-N)Cl][Cl] [N-N = en (**4**) and dach (**5**)] in fair to very good yields (Scheme 1). The corresponding PF_6^- salts were obtained by the addition of excess NH_4PF_6 to ethanol solutions of the chloride salts. The preparation of the corresponding dicationic derivatives *mer*-[Ru(L_3)(N-N)(dmso-*S*)][Y]$_2$ (**6**−**10**; Y = PF_6 or CF_3SO_3), in which the Cl ligand is replaced by a dmso molecule, was performed by two alternative methods (Scheme 1): either by Cl/dmso replacement on the parent chlorido derivatives (assisted by the addition of $AgCF_3SO_3$) or by treatment of the ruthenium(II) precursors **P3** or **P4** with N-N in the presence of NH_4PF_6. We found that with the second method

dx.doi.org/10.1021/ic5005215 | *Inorg. Chem.* 2014, 53, 6113−6126

isolation of the product in pure form often requires purification steps that reduce the yield.

All new complexes were characterized by 1D (^{1}H and ^{13}C) and 2D (^{1}H−^{1}H COSY, ^{1}H−^{13}C HSQC, and ^{1}H−^{13}C HMBC) NMR, IR, and UV spectroscopy and elemental analysis.

The ^{1}H and ^{13}C NMR spectra of **1** in CD_3NO_2 are consistent with a C_s symmetry in solution due to the conformational mobility of the en backbone that averages it to a planar ligand. In the ^{1}H NMR spectrum, there are five aromatic resonances assigned to the equal halves of Cl-tpy and three resolved upfield multiplets attributed to the en ligand. The fourth, and most upfield, en resonance, which overlaps with the broad HOD peak and is evident in the ^{1}H−^{1}H COSY NMR spectrum (Figure S1 in the SI) was assigned to the NH_2 protons that fall into the shielding cone of the adjacent Cl-tpy ligand. The ^{13}C NMR spectrum displays eight resolved resonances in the downfield region for the aromatic carbon atoms and two, partially overlapped, upfield resonances assigned to the en carbon atoms. The assignment of the quaternary carbon atoms (C2′/C6′, C2/C2″, and C4′) was achieved by the long-range 2D heteronuclear ^{1}H−^{13}C HMBC NMR experiment (Figure S1 in the SI).

Conversely, the ^{1}H and ^{13}C NMR spectra of **2** in CD_3NO_2 are more complicated due to the conformational rigidity of coordinated dach[19c,31] that removes the mirror plane bisecting the Cl-tpy ligand in **1**. Thus, in the ^{1}H NMR spectrum, the resonances of the corresponding protons in the halves of Cl-tpy are partially overlapped except for H6/H6″ (two doublets at δ 8.98 and 8.93) and H3′/H5′ (two doublets at δ 8.39 and 8.36), which are well-resolved (Figure S2 in the SI). Similarly, in the ^{13}C NMR spectrum, each carbon atom of Cl-tpy and dach has a resolved resonance (Figure S2 in the SI).

The ^{1}H NMR spectrum of **3** in D_2O (where, unlike **1** and **2**, it is sufficiently stable) is consistent with the symmetry of the complex: five resonances attributed to the symmetric Cl-tpy ligand and eight multiplets assigned to the inequivalent halves of bpy (Figure 2). It is worth noting that each peak of the axial bpy ring is remarkably shifted upfield compared to that of the corresponding proton on the other ring [e.g., δ(Hi) 6.95 vs δ(Hb) 7.99] due to the shielding effect of Cl-tpy. Correspondingly, the protons of the terminal aromatic rings of Cl-tpy are affected by the shielding cone of bpy, and their resonances are also remarkably upfield-shifted; in particular, the H6/H6″ protons resonate at δ 7.79, that is, ca. δ 1.00 more upfield compared to **1** and **2**.

The ^{1}H (Figure S3 in the SI) and ^{13}C NMR spectra of **4** and **5** in CD_3NO_2 are similar to those of **1** and **2**, respectively, with the expected differences due to the presence of a proton in position H4′ instead of the chloride.

The ^{1}H (and ^{13}C) NMR spectra of complexes **6**−**10**, in either D_2O or deuterated acetone, are very similar to those of the corresponding chlorido derivatives, with the obvious presence of the dmso-*S* resonance: a singlet in **6**, **8**, and **9** and two equally intense singlets for the diasterotopic methyl groups in the less symmetrical dach complexes **7** and **10** (Figure S4 in the SI). In all compounds, the dmso-*S* resonance is remarkably upfield-shifted (δ 2.50−2.55) compared to its typical chemical shift range (i.e., from δ 3.00 to 4.00) because the methyl groups fall into the shielding cone of the tpy aromatic rings. Interestingly, replacement of Cl by dmso-*S* induces a remarkable downfield shift ($\Delta\delta \approx 1.30$) of the resonances of the axial NH_2 protons of en and dach.

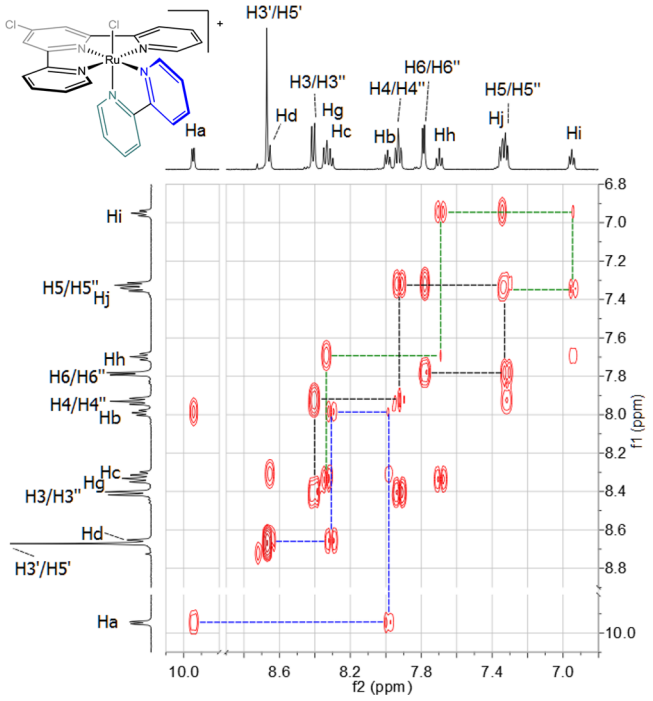

Figure 2. Downfield region of the ^{1}H−^{1}H COSY NMR spectrum of $\mathbf{3}_{Cl}$ in D_2O at 298 K (for the numbering scheme, see Figure 1).

The molecular structures of the cationic compound $\mathbf{3}_{Cl}$ (Figure 3) and of the dicationic complexes [Ru(Cl-tpy)(en)(dmso-*S*)][Y]$_2$ [Y = PF_6 ($\mathbf{6}_{PF_6}$), Figure 4; Y = CF_3SO_3 ($\mathbf{6}_{OTf}$), Figure S5 in the SI)] and $\mathbf{8}_{OTf}$ (Figure 5) were determined in the solid state by X-ray crystallography. The structure of [Ru(tpy)(dach)(dmso-*S*)][PF_6]$_2$ ($\mathbf{10}_{PF_6}$) was also confirmed by X-ray crystallography (Figure S6 in the SI); however, because of the low quality of the crystals, no crystal data are reported for this analysis. In all structures, the ruthenium ion displays the

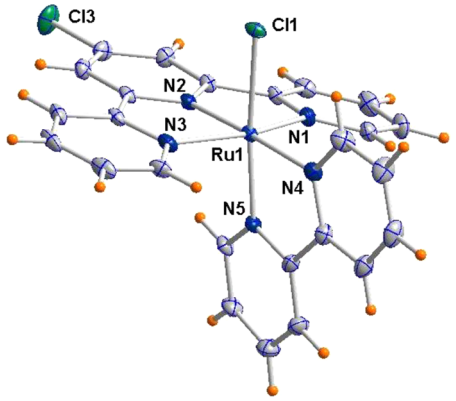

Figure 3. Molecular structure (ORTEP view; thermal ellipsoids at the 50% probability level) of one of the two independent cations of $\mathbf{3}_{Cl}$ with a heteroatom labeling scheme. Selected bond lengths (Å) and angles (deg) for the molecule shown: Ru1−N1 2.067(3), Ru1−N2 1.953(3), Ru1−N3 2.064(3), Ru1−N4 2.079(3), Ru1−N5 2.032(3), Ru1−Cl1 2.4205(9); N3−Ru1−N1 158.84(12), N2−Ru1−N4 177.28(12), N5−Ru1−Cl1 172.05(9). Selected bond lengths (Å) and angles (deg) for the molecule not shown: Ru2−N6 2.072(3), Ru2−N7 1.961(3), Ru2−N8 2.065(3), Ru2−N9 2.084(3), Ru2−N10 2.031(3), Ru2−Cl2 2.4162(9); N8−Ru2−N6 158.89(12), N7−Ru2−N9 176.53(12), N10−Ru2−Cl2 172.09(9).

dx.doi.org/10.1021/ic5005215 | *Inorg. Chem.* 2014, 53, 6113−6126

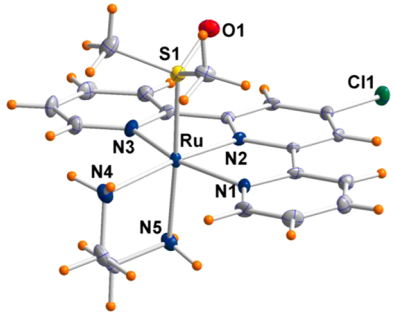

Figure 4. Molecular structure (ORTEP view; thermal ellipsoids at the 50% probability level) of the cation of complex [Ru(Cl-tpy)(en)(dmso-*S*)][PF_6]$_2$ ($\mathbf{6}_{PF_6}$) with a heteroatom labeling scheme. Selected bond lengths (Å) and angles (deg): Ru−N1 2.087(3), Ru−N2 1.967(3), Ru−N3 2.092(3), Ru−N4 2.162(4), Ru−N5 2.146(3), Ru−S1 2.2453(11); N1−Ru−N3 159.17(15), N2−Ru−N4 171.94(13), N5−Ru−S1 177.30(9).

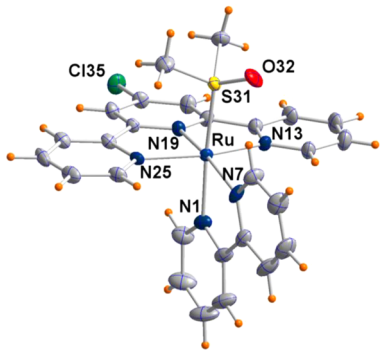

Figure 5. Molecular structure (ORTEP view; thermal ellipsoids at the 50% probability level) of the cation of complex $\mathbf{8}_{OTf}$ with a heteroatom labeling scheme. Selected bond lengths (Å) and angles (deg): Ru−N13 2.083(7), Ru−N19 1.971(7), Ru−N25 2.078(7), Ru−N1 2.097(7), Ru−N7 2.126(6), Ru−S31 2.268(2); N13−Ru1−N25 158.9(3), N7−Ru1−N19 170.1(3), N1−Ru1−S31 175.2(2).

typical distorted octahedral geometry with the tridentate Cl-tpy or tpy ligand coordinated with the expected meridional geometry, the N-N donor as the chelating ligand, and the sixth coordination site occupied either by a chloride ion (in $\mathbf{3}_{Cl}$) or by a dmso molecule bonded through sulfur (in **6**, **8**, and **10**). The asymmetric unit of $\mathbf{3}_{Cl}$ comprises two crystallographically independent complex molecules having closely comparable geometry. Two crystallographically independent complex molecules that slightly differ in the orientation of the dmso molecule with respect to the equatorial plane of Cl-tpy were also found in the asymmetric unit of $\mathbf{6}_{OTf}$ (Figure S5 in the SI).

The complex cations of $\mathbf{3}_{Cl}$ and $\mathbf{8}_{OTf}$ show comparable structural features, with the central nitrogen atom of Cl-tpy having the shortest Ru−N distance (mean value 1.96 Å), as expected because of the geometrical constraints of the tridentate ligand. In contrast, the Ru−N(Cl-tpy) bond distances in the trans position average to 2.071 Å. The coordination bond lengths of the pyridyl rings of bpy are influenced by the nature of the monodentate ligand (and thus by the total charge of the complex): the Ru−N(bpy) bond length trans to Cl^- is significantly shorter than that trans to dmso-*S* [2.097(7) vs 2.031(3) Å, mean value for the latter], and the same tendency is manifested also by the equatorial Ru−N(bpy) bond [2.126(6) Å in $\mathbf{8}_{OTf}$ vs 2.082(3) Å mean value in $\mathbf{3}_{Cl}$]. The planes of chelating Cl-tpy/bipy ligands are almost orthogonal, forming dihedral angles of 81.12(5) and 84.15(5)° in the two complexes of $\mathbf{3}_{Cl}$ and of 86.40(1)° in $\mathbf{8}_{OTf}$. Overall, the geometrical features of $\mathbf{3}_{Cl}$ and $\mathbf{8}_{OTf}$ are comparable to those found in the corresponding tpy derivatives [Ru(tpy)(bpy)Cl][PF_6] and [Ru(tpy)(bpy)(dmso-*S*)][CF_3SO_3]$_2$.[32,33]

In the en derivatives $\mathbf{6}_{PF_6}$ and $\mathbf{6}_{OTf}$, the cation presents a similar coordination environment with Ru−N(Cl-tpy) bond lengths comparable to those of the bpy compound $\mathbf{8}_{OTf}$. Slightly longer Ru−N distances, typical for Ru−N_{sp3} bonds, are observed in the en ligand: 2.162(4) and 2.146(3) Å in $\mathbf{6}_{PF_6}$ and in the range of 2.125(4)−2.148(4) Å for the two independent cations of $\mathbf{6}_{OTf}$, with the shortest values being those located trans to dmso-*S*. The Ru−S distances are sensibly longer in the case of $\mathbf{8}_{OTf}$ compared to **6** [e.g., 2.268(2) Å in $\mathbf{8}_{OTf}$ vs 2.241(1)/2.238(1) Å in $\mathbf{6}_{OTf}$]. This trend is consistent with dmso-*S* being a moderate π acceptor and with en being a better σ donor than bpy (which, in addition, is also a π acceptor).

The solid-state IR spectra of all new complexes show the typical bands of the terpyridine ligands, with the most characteristic being a strong band in the region 1594−1616 cm^{-1} assigned to ν(C=N) stretching.[32] All of the dicationic complexes (**6** − **10**) display bands in the region 1106−1071 cm^{-1}, typical for the S=O stretching of dmso-*S*, and in the region 430−419 cm^{-1}, assigned to the Ru−S_{dmso} stretching.[24,33] The presence of $CF_3SO_3^-$ as a counterion is confirmed by two strong peaks at ca. 1250 and 1025 cm^{-1} and two at ca. 1223 and 1163−1145 cm^{-1} for the SO_3 and CF_3 stretching modes, respectively,[19d,34] and that of PF_6^- by the very strong peaks at 844−833 cm^{-1} and at ca. 558 cm^{-1}.[19c,35]

The electronic absorption spectra of the new complexes exhibited several intense bands in the UV region (200 < λ <

Scheme 2. Chemical Behavior of Complexes 1−5 in Aqueous Solution

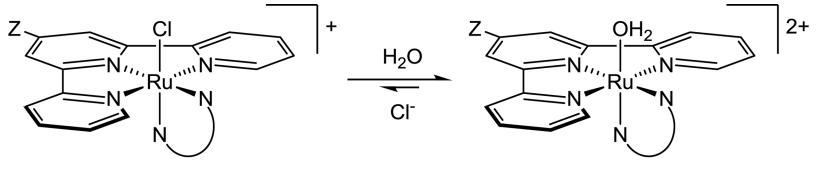

Z = Cl	Z = H	N N	Z = Cl	Z = H
1	4	en	1aq	4aq
2	5	dach	2aq	5aq
3		bpy	3aq	

dx.doi.org/10.1021/ic5005215 | *Inorg. Chem.* 2014, 53, 6113−6126

Table 1. Rate Constants for the Aquation and Half-lives at 298 K in Water and Buffer Solution for Compounds 1 and 2

		water		buffer[a]	
compound	isosbestic points [nm]	k_{H_2O} [$\times 10^{-3}$ s^{-1}]	$(t_{1/2})_{H_2O}$ [min]	k_{H_2O} [$\times 10^{-3}$ s^{-1}]	$(t_{1/2})_{H_2O}$ [min]
1	347, 416, 491	2.52 ± 0.01	4.58 ± 0.03	2.82 ± 0.01	4.10 ± 0.03
2	424, 500, 532, 557	3.94 ± 0.02	2.93 ± 0.02	4.00 ± 0.02	2.90 ± 0.02

[a]In 25 mM Hepes buffer, pH = 7.4.

330 nm), attributed to intraligand ($\pi \rightarrow \pi^*$) charge-transfer transitions, and a broad intense band (with an unresolved shoulder in cases of **1**−**5**) in the visible region attributed to metal-to-ligand $d\pi(Ru) \rightarrow \pi^*$(polypyridyl) charge-transfer transitions.[26,32a,b,36] The absorption maximum of the latter band is strongly influenced by the charge: replacement of Cl^- by dmso induces a blue shift from ca. 500 nm in **1**−**5** to ca. 420 nm in **6**−**10**.[24,33b,c]

Chemical Behavior in Aqueous Solution. Contrary to what was previously observed for most polypyridylruthenium terpyridine compounds, our new complexes are well soluble in water (in particular, the chloride salts, >25 mg/mL), with the exception of the dicationic bpy compound **8** (both as OTf^- and as PF_6^- salt), which has limited solubility (ca. 5 mg/mL).

NMR Investigation. The behavior of the new complexes in aqueous solution, which is of great importance for compounds with potential antitumor activity, was first investigated qualitatively by NMR spectroscopy. The chloride ligand in the cationic compounds **1** and **2** turned out to be very labile in aqueous solution. Immediately after dissolution in D_2O, a new set of resonances was observed to grow both in the aromatic (Cl-tpy resonances) and in the upfield (en or dach resonances) regions of the ^1H NMR spectra. These new resonances, which grew at the expense of those of the parent compound, were attributed to the aqua species $[Ru(Cl\text{-}tpy)(en)(OH_2)]^{2+}$ (**1aq**) and $[Ru(Cl\text{-}tpy)(dach)(OH_2)]^{2+}$ (**2aq**), respectively (Scheme 2). In particular, according to integration, 40% of **1** is already aquated 2 min after dissolution, and the system reached equilibrium within ca. 1 h with a 1:9 ratio between **1** and **1aq** (Figure S7 in the SI). The addition of a large excess of NaCl (ca. 1.00 M) to this solution induced rapid reversion of the equilibrium toward the parent compound **1** and eventually to its partial precipitation (as a Cl salt). The chemical behavior in aqueous solution of the dach derivative **2**, and of the corresponding tpy compounds **4** and **5**, is similar to that described for **1**.

Conversely, the bpy compound **3** releases the Cl^- ligand, yielding the aqua species $[Ru(Cl\text{-}tpy)(bpy)(OH_2)]^{2+}$ (**3aq**) at a much slower rate (even though eventually to a comparable extent). The equilibrium was, in fact, reached ca. 8 h after dissolution. The addition of a large excess of NaCl to the equilibrated solution induced rapid precipitation of the chlorido derivative **3**.

The greater lability of the Cl^- ligand in compounds **1** and **2** is attributed to the stronger trans influence of the pure σ-donor ligands en and dach, respectively, compared to the (also) π-acceptor bpy in compound **3**.

Contrary to that observed for the chlorido derivatives, the dicationic dmso derivatives **6**−**10** are very stable in aqueous solution; their NMR spectra in D_2O remained unchanged for several hours after dissolution, and no release of dmso was observed. This finding is consistent with a strong Ru−S bond (notwithstanding the 2+ charge) due to the presence of a good σ-donor ligand (en and dach) trans to dmso.

Kinetics of Aquation. The kinetics of aquation of compounds **1** and **2** were quantitatively studied by UV/visible spectroscopy at 298 K on 0.1 mM solutions. From the NMR data, complexes **4** and **5** are expected to have similar kinetics, whereas compound **3** hydrolyzes the Cl ligand at a much slower rate. The rapid reversion of the equilibrium and the partial precipitation of the complexes upon the addition of NaCl prohibited anation kinetic studies and, therefore, calculation of the equilibrium constants K_{aq}.

The UV/visible spectra of both compounds show significant time-dependent changes in the region 200−800 nm (Figure S8 in the SI) with clean isosbestic points that, consistent with the NMR observation, suggest the occurrence of a single hydrolytic process (i.e., conversion of the initial chlorido complex into the corresponding aqua species **1aq** and **2aq**, respectively). The wavelength corresponding to the maximum change in absorption (Figure S8 in the SI, difference spectra) was selected for the kinetic studies (464 nm for **1** and 476 nm for **2**). In each case, the time course of the absorbance followed first-order kinetics (Figure S9 in the SI), which afforded the rate constants k_{H_2O} listed in Table 1. The en complex **1** hydrolyzes about 1.5 times slower than the dach complex **2**. Similar results were obtained when aquation of the complexes occurred in a buffer solution (25 mM Hepes buffer; pH = 7.4; Table 1 and Figure S9 in the SI). It is worth noting that the aquation rates of **1** and **2** are slightly faster than those of the anticancer active half-sandwich organometallic compounds $[Ru(\eta^6\text{-arene})(en)Cl][PF_6]$ [$(1.23-2.26) \times 10^{-3}$ s^{-1}][37] and ca. 2 orders of magnitude higher than those of the established anticancer drug cisplatin (6.32×10^{-5} and 2.5×10^{-5} s^{-1} for the first and second aquation processes, respectively).[38]

pK_a Determinations. With the aim of assessing whether the complexes **1**−**3** are present as the aqua adducts or as the less reactive hydroxo species in physiological conditions (i.e., pH = 7.2−7.4), pH titrations were performed on the aqua species **1aq**−**3aq**. Their NMR spectra showed significant changes upon variation of the pH from 2 to 13. For each species, the resonance that showed the largest pH-dependent variation of the chemical shift was selected for analysis: the most upfield NH resonance for **1aq** and **2aq** and the singlet assigned to C3′*H*/C5′*H* for **3aq**. As the pH was increased, those peaks shifted upfield, as shown in Figure S10 in the SI. Analysis of the NMR titration curves gave pK_a values of 10.50 ± 0.03, 10.26 ± 0.02, and 9.56 ± 0.01 for species **1aq**−**3aq**, respectively (Figure S11 in the SI). The latter value is closely comparable to that reported for the corresponding tpy complex, i.e., $[Ru(tpy)(bpy)(OH_2)]^{2+}$ ($pK_a \approx 9.7$).[36a] It can be seen that deprotonation of the aqua ligand is influenced by the nature of the N-N chelating ligand: the presence of the aromatic bpy ligand makes the aqua ligand slightly more acidic, whereas replacement of en by dach has little influence. However, the obtained pK_a values clearly indicate that all complexes **1**−**3** are largely in the reactive aqua form once dissolved in a medium with physiological pH; only ca. 0.15% of **1aq** and **2aq** and ca.

dx.doi.org/10.1021/ic5005215 | Inorg. Chem. 2014, 53, 6113−6126

0.75% of **3aq** are calculated to be in the hydroxo form at pH = 7.4.

Interaction with Guanine Derivatives. The reactivity of compounds **1**−**3** toward two guanine derivatives, i.e., 9MeG and 5′-GMP, as model DNA bases, was investigated primarily by ^{1}H and ^{31}P NMR spectroscopy in D_2O at ambient temperature (for the numbering scheme of 9MeG and 5′-GMP, see the corresponding figures in the SI). The assignment of selected resonances of the products is reported in Table S2 in the SI.

The addition of a slight excess of 9MeG (1.3 equiv) to an equilibrated solution of **1** (4 mM, pH = 7.78) in D_2O induced relatively fast changes in the ^{1}H NMR spectrum (Figure S12 in the SI). A new set of resonances attributed to the product [Ru(Cl-tpy)(en)(9MeG-N7)]$^{2+}$ (**11**) started to grow within minutes. Although binding of a ruthenium(II) center to N7 of purine moieties typically induces a downfield shift of the H8 resonance compared to the free ligand,[16,20,39] in our case, binding of **1** to N7 of 9MeG led to a remarkable upfield shift of the H8 singlet (δ 6.20 vs 7.77; $\Delta\delta$ = −1.57) because of the shielding effect of the adjacent Cl-tpy. A similar shift, even though less pronounced, was observed for the CH_3 singlet (δ 3.18 vs 3.68). The same behavior was detected for all studied systems, either with 9MeG or 5′-GMP, and will not be commented on further. Quantitative formation of **11** occurred within ca. 3 h, and no spectral changes were observed afterward.

Similarly, the reaction of **1** with 5′-GMP (1:1, 10 mM, D_2O, pH = 7.03) yielded quantitatively one final product that was identified by ^{1}H (Figure S13 in the SI) and ^{31}P (Figure S14 in the SI) NMR spectroscopy as the N7-bonded neutral species [Ru(Cl-tpy)(en)(5′-GMP-N7)] (**12**). The reaction is relatively fast, as indicated by the rapid appearance of the signals of **12** immediately after mixing; 100% conversion occurred within ca. 2 h, and no spectral changes were observed afterward. Interestingly, each Cl-tpy peak is split into two equally intense resonances (partially overlapped except for H6/H6″): the stereogenic center of coordinated 5′-GMP causes a loss of the symmetry plane that makes the halves of Cl-tpy equivalent in **1** (and in **1aq**). In the ^{31}P NMR spectrum, consistent with the ^{1}H NMR findings, only a new singlet grew during the reaction time and was assigned to **12** (Figure S14 in the SI). Indeed, the new resonance is slightly shifted to higher frequency (δ 3.31) compared to that of free 5′-GMP (δ 2.99), which is typical for N7 binding.[16,20] It is worth noting that no transient intermediates, such as those reported for the half-sandwich active compounds (e.g., oxygen binding to the phosphate group of 5′-GMP),[16,20] were detected.

To verify the identity of products **11** and **12**, i.e., that binding of guanine derivatives on the {Ru(Cl-tpy)(en)}$^{2+}$ fragment occurs through N7, pH titrations were carried out on the solutions after the accomplishment of each reaction and, for comparison, on equimolar solutions of the free nucleobases. The pH dependence was monitored by the shift of the H8 singlet in the ^{1}H NMR spectra and by the PO_3H resonance in ^{31}P NMR spectra, which are particularly sensitive to protonation of N7 and deprotonation of the phosphate group, respectively. The ^{1}H and ^{31}P NMR titration curves are shown in Figure 6 amd Figure S15 in the SI; the pK_a values, determined by computer fits of the Henderson−Hasselbalch equation, are reported in Table 2. Two pK_a values were determined for free 9MeG, 9.90 and 2.88, attributable to deprotonation of N1H and protonation of N7, respectively, whereas three values were obtained in the case of free 5′-GMP,

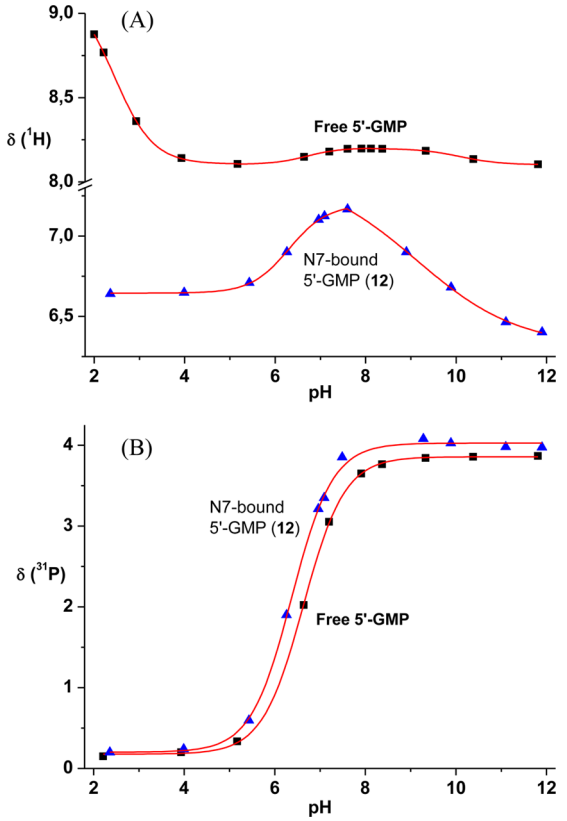

Figure 6. Plots of the pH dependence of the H8 (A) and phosphate (B) NMR resonances for free 5′-GMP (■) and **12** (▲) at ambient temperature. The curves are computer-fitted (red lines), yielding the pK_a values listed in Table 2.

Table 2. pK_a Values for 9MeG and 5′-GMP and Their {Ru(Cl-tpy)(en)}$^{2+}$ Adducts at Ambient Temperature

species	group	pK_a (^{1}H)	pK_a (^{31}P)
9MeG	N7	2.88 ± 0.10	
	N1H	9.90 ± 0.26	
11	N1H	9.47 ± 0.10	
5′-GMP	N7	2.44 ± 0.04	
	$-OP_3H$	6.71 ± 0.04	6.63 ± 0.01
	N1H	10.09 ± 0.02	
12	$-OP_3H$	6.31 ± 0.02	6.37 ± 0.03
	N1H	9.12 ± 0.15	

10.09, 6.71, and 2.44, attributable to deprotonation of N1H and PO_3H and protonation of N7, respectively. Our experimental values are closely comparable with those determined by others.[40] From the titration curves, it can be seen that compound **11** undergoes deprotonation of N1H (pK_a of 9.47) but no protonation of N7 (Figure S15 in the SI). Similarly, complex **12** undergoes deprotonation only of PO_3H (pK_a of 6.31) and N1H (pK_a of 9.12) (Figure 6). These observations provide clear evidence that the guanine derivatives bind to the ruthenium center through N7.

Similar results were obtained with [Ru(Cl-tpy)(dach)Cl]$^{+}$ (**2**), with quantitative formation of [Ru(Cl-tpy)(dach)(9MeG-N7)]$^{2+}$ (**13**) in ca. 2 h (Figure S16 in the SI) and of [Ru(Cl-tpy)(dach)(5′-GMP-N7)]$^{2+}$ (**14**) in ca. 1 h (Figure S17 in the SI). Compound **14**, due to the conformational rigidity of coordinated dach and to the stereogenic center on 5′-GMP, is obtained as a pair of two equally abundant diastereomers

dx.doi.org/10.1021/ic5005215 | Inorg. Chem. 2014, 53, 6113−6126

(Figure S18 in the SI). Many proton resonances are partially overlapped, but two resolved singlets for H8 (δ 6.57 and 6.54) and four doublets for H6/H6″ (δ 9.08, 9.03, 8.93, and 8.88) were clearly observed. When the reaction leading to **14** was monitored by ^{31}P NMR spectroscopy, only one new peak (δ 3.37) was detected, even though, in principle, two singlets would be expected for the two diastereomers (Figure S19 in the SI). We speculate that their chemical shifts are too close to be resolved, consistent with the PO_3H group being far from the stereogenic centers.

Contrary to **1** and **2**, the reaction of $[Ru(Cl\text{-}tpy)(bpy)Cl]^+$ (**3**) (1:1, 4 mM, pH = 6.87) with 9MeG is very slow: a new set of resonances, attributable to $[Ru(Cl\text{-}tpy)(bpy)(9MeG\text{-}N7)]^{2+}$ (**15**), became apparent in the ^{1}H NMR spectrum within the first hours. The system reached equilibrium after ca. 5 days, with ca. 45% of 9MeG bound to ruthenium (i.e., **15**), 50% of **3aq**, and 5% of **3** (Figure S20 in the SI).

The reaction of **3** with 5′-GMP (1:1, 10 mM, pH = 7.23) is also very slow compared to those of **1** and **2**. More specifically, 20 min after the addition of 5′-GMP to an equilibrated solution of **3** the growth of a new set of resonances, assignable to $[Ru(Cl\text{-}tpy)(bpy)(5'\text{-}GMP\text{-}N7)]^{2+}$ (**16**), was observed in the ^{1}H NMR spectrum (Figure S21 in the SI). The system reached equilibrium after ca. 24 h, and the distribution of the species was ca. 40% of **16**, 47% of **3aq**, and 13% as **3**. Consistent with the ^{1}H NMR data, only one new peak (δ 3.45) was detected in the ^{31}P NMR spectrum during the time course of the reaction.

The above NMR evidence clearly shows that complexes **1** and **2**, with an aliphatic diamine as the chelating ligand, react with 9MeG and 5′-GMP much faster compared to the bpy complex **3**. In addition, the reactions of **1** and **2** with the model bases are quantitative, whereas those of **3** are not. The fact that Ru^{II}-tpy complexes with pyridyl ligands are rather sluggish in their reactions toward model DNA bases has also been observed previously. For example, the partial reaction of $[Ru(tpy)(Me_2bpy)Cl]^+$ with 5′-GMP required ca. 4 h at 310 K, and only 20% of $[Ru(tpy)(apy)(9EtG\text{-}N7)]^{2+}$ (9EtG = 9-ethylguanine) is formed after 5 h at 310 K when $[Ru(tpy)(apy)(H_2O)]^{2+}$ is treated with 9EtG.[11,13a]

Interaction of $[Ru(Cl\text{-}tpy)(en)Cl]^+$ (1) with 5′-AMP and Competitive Reaction with a Mixture of 5′-AMP and 5′-GMP. To investigate the binding preference of the new complexes toward nucleobases, we studied the interaction of **1** with an adenosine derivative, i.e., 5′-AMP, as well as the reaction of **1** with 5′-GMP in competition with 5′-AMP. These reactions were investigated by ^{1}H and ^{31}P NMR spectroscopy in D_2O at ambient temperature (for the numbering scheme of 5′-AMP, see Figure S22 in the SI).

The addition of an equilibrated solution of **1** to a solution of 5′-AMP (C_{final} = 10 mM, 1:1, D_2O, pH = 7.00) gave rise to rapid, but relatively minor, changes in the NMR spectrum (Figure S22 in the SI). Many new resonances appeared immediately after mixing, and an equilibrium was reached within 1 h. Overall, according to integration, less than 10% of the reactants were transformed into the new species. No assignment of the new resonances was attempted. The ^{31}P NMR spectrum, consistent with the ^{1}H NMR data, showed the formation of new minor species, as indicated by the broadening, due to the partial overlap of the new resonances, of the peak of free 5′-AMP (δ 3.04). These results clearly indicate that **1** has a minor affinity for 5′-AMP. Indeed, in a competition reaction with a 1:1 mixture of 5′-AMP and 5′-GMP, complex **1** showed a large preference toward 5′-GMP. More specifically, the exclusive formation of **12** was observed within the first hours after the addition of **1aq** to a solution containing equimolar amounts of both 5′-AMP and 5′-GMP (C_{final} = 10 mM, 1:1, D_2O, pH = 7.07), as evidenced by ^{1}H (Figure S23 in the SI) and ^{31}P (Figure S24 in the SI) NMR spectroscopy.

UV/Visible Studies of the Reaction of Compounds 1 and 2 with Guanine Derivatives. The kinetics of the reactions of complexes **1** and **2** with 9MeG and 5′-GMP were determined spectrophotometrically (Figure S25 in the SI) by following the change in absorbance at selected wavelengths, corresponding to the maximum change (Figure S26 in the SI, difference spectra), as a function of time. All kinetic experiments were performed under pseudo-first-order conditions with respect to the nucleophile. To suppress spontaneous hydrolysis of the chloride from ruthenium, experiments were performed in the presence of 30 mM NaCl. This value was determined prior to kinetic measurements as the minimum chloride concentration for which no spectral changes were observed (Figure S27 in the SI).

The substitution reactions of complexes **1** and **2** with guanine derivatives can be represented by eq 2

$$[Ru(Cl\text{-}tpy)(N\text{-}N)Cl]^+ + L \underset{k_1}{\overset{k_2}{\rightleftharpoons}} [Ru(Cl\text{-}tpy)(N\text{-}N)L]^n + Cl^- \quad (2)$$

where N-N = en or dach, L = 9MeG or 5′-GMP, and n = +2 or 0 depending the charge of the entering ligand.

Here, k_2 is the second-order rate constant for the forward reaction, involving the direct attack of the nucleophile L, and k_1 is the rate constant for the reverse reaction. The second-order rate constants k_2 are obtained directly from the slopes of the plots of k_{obsd} versus the concentration of entering nucleophile, whereas the k_1 values are derived from the intercepts divided by

Table 3. Rate Constants and Activation Parameters for the Substitution Reactions between Complexes 1 and 2 with 5′-GMP and 9MeG (25 mM Hepes Buffer, 30 mM NaCl, pH = 7.4)

	T [K]	k_2 [$\times 10^{-1}$ M^{-1} s^{-1}]	k_1 [$\times 10^{-3}$ M^{-1} s^{-1}]	$\Delta H_2^{\ddagger}$ [kJ mol^{-1}]	$\Delta S_2^{\ddagger}$ [J K^{-1} mol^{-1}]
			1		
5′-GMP	298	1.5 ± 0.1	4.9 ± 0.9	69 ± 3	−45 ± 10
	310	4.7 ± 0.3	16.0 ± 3.0		
	318	8.8 ± 0.2	30.0 ± 2.0		
9MeG	310	1.3 ± 0.1	4.1 ± 0.8		
			2		
5′-GMP	298	3.3 ± 0.2	1.8 ± 0.2	51 ± 3	−101 ± 9
	310	7.1 ± 0.2	3.0 ± 0.2		
	318	12.6 ± 0.6	4.7 ± 0.7		
9MeG	310	3.1 ± 0.2	10.0 ± 2.0		

$[Cl^-]$ (i.e., 30 mM). Their values are listed in Table 3. The rate of the reaction is described by eqs 3 and 4.

$$-\frac{d[Ru(Cl\text{-}tpy)(N\text{-}N)Cl]^+}{dt} = k_{obsd}[Ru(Cl\text{-}tpy)(N\text{-}N)Cl]^+ \quad (3)$$

$$k_{obsd} = k_1[Cl^-] + k_2[L] \quad (4)$$

All kinetic runs could be fitted by a single-exponential function, and no subsequent reaction was observed. Each pseudo-first-

dx.doi.org/10.1021/ic5005215 | Inorg. Chem. 2014, 53, 6113−6126

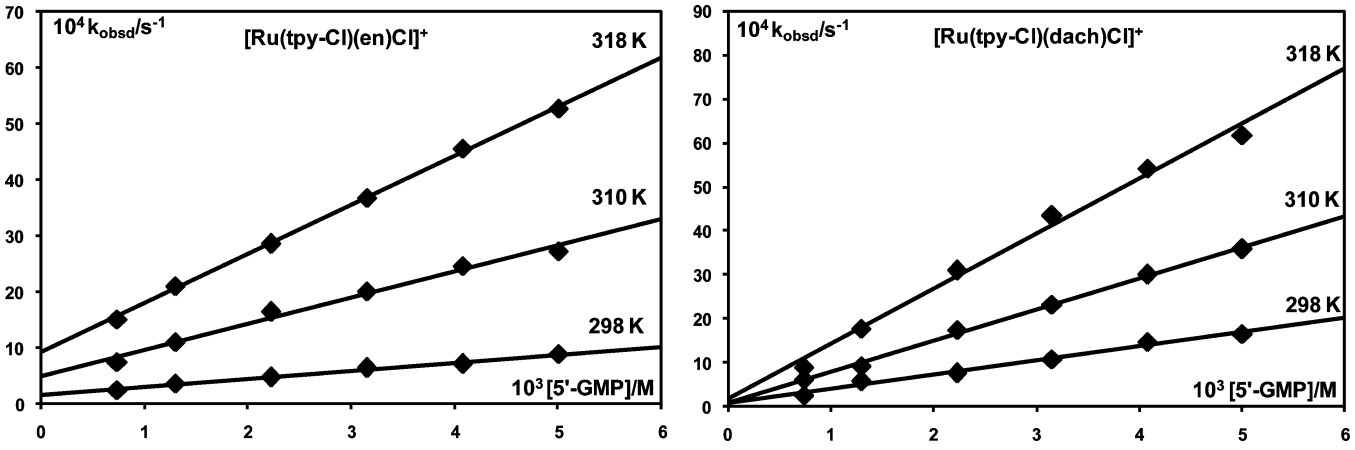

Figure 7. Pseudo-first-order rate constants, k_{obsd}, as a function of the ligand concentration and temperature for the substitution reactions of **1** (left) and **2** (right) with 5′-GMP in 25 mM Hepes buffer (30 mM NaCl, pH = 7.4).

order rate constant, k_{obsd}, was calculated as the average value of two or three independent runs (Tables S3−S6 in the SI).

The experimental results for the substitution reactions of the two complexes with 9MeG and 5′-GMP (at three different temperatures) are shown in Figure S28 in the SI and Figure 7, respectively. A linear dependence on the nucleophile concentration was observed for all reactions. The activation parameters ($\Delta H^{\ddagger}$ and $\Delta S^{\ddagger}$), obtained from the Eyring plots, are summarized in Table 3. The small values of $\Delta H^{\ddagger}$ and negative values of $\Delta S^{\ddagger}$ clearly support the associative mechanism for the substitution process. Similar mechanisms have been proposed for the substitution reactions of organometallic ruthenium arene complexes and of half-sandwich Ru-[9]aneS3 coordination compounds studied in our previous work with biologically relevant ligands, e.g., 9MeG, guanosine (Guo), 5′-GMP, L-histidine (L-His).[20,41]

It can be seen that the rate constants depend on the nature of the chelating ligand and on the charge of the entering ligand: complex **2** reacts from 1.5 to 2.5 times faster than complex **1**, and the reactions with 5′-GMP occur 2.3−3.7 times faster than with 9MeG (Table 3), most likely because it has more favorable electrostatic interactions with the cationic complexes. For comparison, the half-sandwich ruthenium(II) coordination compounds with the general formula [Ru([9]aneS3)(N-N)Cl][PF_6] have k_2 values that are ca. from 1.2 to 4 times smaller than those of **1** and **2** for the reaction with 5′-GMP under the same conditions.[20]

CONCLUSIONS

Whereas monofunctional ruthenium(II) complexes of the type $[Ru(L_3)(N\text{-}N)X]^n$ with facial geometry have been widely investigated for their antitumor activity and some structure−activity relationship rules are already established, those with a meridional geometry are almost neglected. The typical tridentate ligand selected for imposing the meridional geometry to the complex is tpy. In most of the Ru^{II}-tpy compounds reported so far in the literature, also N-N is a polypyridyl ligand (e.g., bpy): as a consequence, the complexes typically suffer from low solubility in aqueous media, limiting biologically relevant investigations. With the aim of contrasting this tendency, we described here the synthesis and structural characterization of a series of new water-soluble, monofunctional ruthenium(II) complexes with meridional geometry of the general formula *mer*-$[Ru(L_3)(N\text{-}N)X][Y]_n$ (where L_3 = Cl-tpy or tpy; N-N = en, dach, or bpy; X = Cl or dmso-*S*; Y = Cl, PF_6, or CF_3SO_3; n = 1 or 2, depending on the nature of X). The chelating ligands en and dach were selected for improving the solubility in water of their complexes and for their capability of forming hydrogen bonds with coordinated nucleobases. This latter property appears as a prerequisite for observing antitumor activity in monofunctional half-sandwich ruthenium(II) compounds. For comparative purposes, the aromatic N-N-donor bpy ligand was also used. With the exception of [Ru(Cl-tpy)(bpy)(dmso-*S*)][Y]$_2$ (**8**, Y = CF_3SO_3 or PF_6), all new complexes are well-soluble in water (>25 mg/mL). Studies on the chemical behavior of the new complexes in aqueous solution, monitored by NMR spectroscopy, showed that the chlorido derivatives **1**−**5** release the Cl^- ligand to form the corresponding aqua species. Whereas the rate of hydrolysis was found to depend markedly on the nature of the chelating ligand (minutes for en and dach and hours for bpy), its extent was similar in all cases, with a ca. 1:9 ratio between intact and aquated species at equilibrium. On the other hand, the dicationic dmso derivatives **6**−**10** were found to be very stable in water; no release of dmso was detected even after several hours of observation. No significant difference was observed between the corresponding tpy and Cl-tpy compounds.

Because DNA is considered to be a potential biological target for metal-based antitumor agents, we investigated the reactivity of **1**−**3** toward the guanine model compounds 9MeG and 5′-GMP. All three complexes bind selectively to N7 of 9MeG and 5′-GMP but with rates and extents that depend strongly on the nature of the chelating ligand: compounds **1** and **2**, which have an aliphatic diamine as the chelating ligand, react much faster (minutes to hours) compared to the bpy complex **3** (days). In addition, the reactions of **1** and **2** are quantitative, whereas those of **3** are not. In no case were intermediates observed. In addition, we established that complex **1** has selectivity for 5′-GMP when competing with 5′-AMP. Not surprisingly, the nature of the bidentate ligand N-N is very relevant in affecting the reactivity of the meridional complexes, since it is trans to the unique reactive coordination position. According to our results, the complexes with the bidentate aliphatic diamines en and dach proved to be clearly superior to those with bpy in terms of solubility and reactivity (i.e., release of Cl and capability to bind guanine derivatives).

Therefore, complexes **1** and **2**, and the similar **4** and **5**, are promising antitumor candidates. In vitro biological evaluation

dx.doi.org/10.1021/ic5005215 | *Inorg. Chem.* 2014, 53, 6113−6126

of their activity is currently underway, and the results will be reported elsewhere.

Given the premise that the relatively rapid availability of one coordination position on the ruthenium center of monofunctional compounds is apparently an essential, even though not unique, requirement for observing anticancer activity, the dmso derivatives **6**−**10** could be considered as inactive. However, a number of inert and coordinatively saturated metal complexes, i.e., compounds that are unable to bind coordinatively to biological targets (*structural compounds*),[6] were shown to display biological activity.[42] Therefore, investigation toward this direction might be of interest.

■ ASSOCIATED CONTENT

Supporting Information

Crystallographic data for $\mathbf{3}_{Cl}$, $\mathbf{6}_{PF_6}$, $\mathbf{6}_{OTf}$ and $\mathbf{8}_{OTf}$ in CIF format, ORTEP drawing of $\mathbf{6}_{OTf}$, molecular structure from low-quality crystal of $\mathbf{10}_{PF_6}$, synthetic procedures for complexes **P1**, **P3**, $\mathbf{1}_{PF_6}$, $\mathbf{2}_{PF_6}$, $\mathbf{4}_{PF_6}$, and $\mathbf{6}_{PF_6}$−$\mathbf{10}_{PF_6}$, NMR spectra of **1**, **2**, **4**, and **5** in CD_3NO_2, ^1H NMR spectra of **6**−**10** in D_2O, time evolution of the ^1H NMR spectrum of **1** in D_2O, time evolution of the UV/visible and UV/visible difference spectra of **1** and **2** in water, time dependence of the absorbance for the aquation of **1** and **2** in water or in buffer, NMR pH titrations for **1aq**−**3aq**, ^1H NMR spectra monitoring the interactions of **1**−**3** with 9MeG and 5′-GMP, ^{31}P NMR spectra monitoring the interaction of **1** with 5′-GMP, ^{31}P NMR spectra of **14** after 1 h, ^1H NMR spectra monitoring the interaction of **1** with 5′-AMP, ^1H and ^{31}P NMR spectra monitoring the competition reaction of **1** with 5′-AMP and 5′-GMP, pH dependence of the H8 ^1H NMR resonance for free 9MeG and for **11**, scheme of conformational isomers of **14**, time evolution of the UV/visible and UV/visible difference spectra of the interaction of **1** and **2** with 9MeG and 5′-GMP, Change of the absorbance at 401 nm of **1** versus [Cl^-], pseudo-first-order rate constants, k_{obsd}, versus [9MeG] for the substitution reactions of **1** and **2** with 9MeG; observed pseudo-first-order rate constants versus [L] and T for the substitution reactions of **1** and **2** with 9MeG and 5′-GMP, assignments of selected ^1H resonances (δ) for the aqua species **1aq**−**3aq** and for complexes **11**−**16**. This material is available free of charge via the Internet at http://pubs.acs.org. CCDC 985412 ($\mathbf{8}_{OTf}$), 985413 ($\mathbf{6}_{OTf}$), 988761 ($\mathbf{6}_{PF_6}$), and 988762 ($\mathbf{3}_{Cl}$) contain the supplementary crystallographic data for this paper. These data can be obtained free of charge at www.ccdc.cam.ac.uk/conts/retrieving.html [or from the Cambridge Crystallographic Data Centre, 12 Union Road, Cambridge CB2 1EZ, U.K.; fax (international) +44-1223/336-033; e-mail deposit@ccdc.cam.ac.uk].

■ AUTHOR INFORMATION

Corresponding Authors

*E-mail: bratsos@chem.demokritos.gr.
*E-mail: alessi@units.it.

Present Address

§I.N.N.: Department of Physical Chemistry, NCSR "Demokritos", 15310 Ag. Paraskevi, Athens, Greece.

Notes

The authors declare no competing financial interest.

■ ACKNOWLEDGMENTS

This work was performed within the frame of COST Action CM1105. Fondazione Beneficentia Stiftung, the Ministry of Science and Technological Development of the Republic of Serbia (Project 172011), and the Slovenian Research Agency (Project J1-4131) are gratefully acknowledged for financial support. A.R. is grateful to the bilateral Italian−Serbian project "C.S.I.U.T." for a research fellowship at the University of Trieste, and J.K. thanks the Slovenian Research Agency for a junior researcher grant. The EN→FIST Centre of Excellence, Ljubljana, Slovenia, is acknowledged for use of the SuperNova diffractometer.

■ REFERENCES

(1) Alessio, E. *Bioinorganic Medicinal Chemistry*; Wiley-VCH Verlag & Co. KGaA: Weinheim, Germany, 2011.
(2) Hartinger, C. G.; Jakupec, M. A.; Zorbas-Seifried, S.; Groessl, M.; Egger, A.; Berger, W.; Zorbas, H.; Dyson, P. J.; Keppler, B. K. *Chem. Biodiversity* **2008**, *5*, 2140−2155.
(3) Rademaker-Lakhai, J. M.; van den Bongard, D.; Pluim, D.; Beijnen, J. H.; Schellens, J. H. M. *Clin. Cancer Res.* **2004**, *10*, 3717−3727.
(4) Gill, M. R.; Thomas, J. A. *Chem. Soc. Rev.* **2012**, *41*, 3179−3192.
(5) Brabec, V.; Nováková, O. *Drug Resist. Updates* **2006**, *9*, 111−122.
(6) Gianferrara, T.; Bratsos, I.; Alessio, E. *Dalton Trans.* **2009**, 7588−7598.
(7) Novakova, O.; Kasparkova, J.; Vrana, O.; van Vliet, P. M.; Reedijk, J.; Brabec, V. *Biochemistry* **1995**, *34*, 12369−12378.
(8) Velders, A. H.; Kooijman, H.; Spek, A. L.; Haasnoot, J. G.; De Vos, D.; Reedijk, J. *Inorg. Chem.* **2000**, *39*, 2966−2967.
(9) van Vliet, P. M.; Toekimin, S. M. S.; Haasnoot, J. G.; Reedijk, J.; Nováková, O.; Vrána, O.; Brabec, V. *Inorg. Chim. Acta* **1995**, *231*, 57−64.
(10) (a) Grover, N.; Gupta, N.; Thorp, H. H. *J. Am. Chem. Soc.* **1992**, *114*, 3390−3393. (b) Neyhart, G. A.; Grover, N.; Smith, S. R.; Kalsbeck, W. A.; Fairley, T. A.; Cory, M.; Thorp, H. H. *J. Am. Chem. Soc.* **1993**, *115*, 4423−4428.
(11) Mulyana, Y.; Collins, G.; Keene, R. *J. Inclusion Phenom. Macrocyclic Chem.* **2011**, *71*, 371−379.
(12) Cheng, C. C.; Lee, W. L.; Su, J. G.; Liu, C. L. *J. Chin. Chem. Soc. (Taipei, Taiwan)* **2000**, *47*, 213−220.
(13) (a) Corral, E.; Hotze, A. C. G.; Magistrato, A.; Reedijk, J. *Inorg. Chem.* **2007**, *46*, 6715−6722. (b) Corral, E.; Hotze, A. C. G.; Den Dulk, H.; Leczkowska, A.; Rodger, A.; Hannon, M. J.; Reedijk, J. *J. Biol. Inorg. Chem.* **2009**, *14*, 439−448.
(14) (a) Gasser, G.; Ott, I.; Metzler-Nolte, N. *J. Med. Chem.* **2011**, *54*, 3−25. (b) Süss-Fink, G. *Dalton Trans.* **2010**, *39*, 1673−1688.
(15) (a) Aird, R. E.; Cummings, J.; Ritchie, A. A.; Muir, M.; Morris, R. E.; Chen, H.; Sadler, P. J.; Jodrell, D. I. *Br. J. Cancer* **2002**, *86*, 1652−1657. (b) Peacock, A. F. A.; Sadler, P. J. *Chem.—Asian J.* **2008**, *3*, 1890−1899. (c) Yan, Y. K.; Melchart, M.; Habtemariam, A.; Sadler, P. J. *Chem. Commun.* **2005**, 4764−4776.
(16) Chen, H.; Parkinson, J. A.; Morris, R. E.; Sadler, P. J. *J. Am. Chem. Soc.* **2003**, *125*, 173−186.
(17) Chen, H.; Parkinson, J. A.; Parsons, S.; Coxall, R. A.; Gould, R. O.; Sadler, P. J. *J. Am. Chem. Soc.* **2002**, *124*, 3064−3082.
(18) Chen, H.; Parkinson, J. A.; Nováková, O.; Bella, J.; Wang, F.; Dawson, A.; Gould, R.; Parsons, S.; Brabec, V.; Sadler, P. J. *Proc. Natl. Acad. Sci. U. S. A.* **2003**, *100*, 14623−14628.
(19) (a) Serli, B.; Zangrando, E.; Gianferrara, T.; Scolaro, C.; Dyson, P. J.; Bergamo, A.; Alessio, E. *Eur. J. Inorg. Chem.* **2005**, 3423−3434. (b) Bratsos, I.; Jedner, S.; Bergamo, A.; Sava, G.; Gianferrara, T.; Zangrando, E.; Alessio, E. *J. Inorg. Biochem.* **2008**, *102*, 1120−1133. (c) Bratsos, I.; Mitri, E.; Ravalico, F.; Zangrando, E.; Gianferrara, T.; Bergamo, A.; Alessio, E. *Dalton Trans.* **2012**, *41*, 7358−7371. (d) Bratsos, I.; Urankar, D.; Zangrando, E.; Genova-Kalou, P.; Košmrlj, J.; Alessio, E.; Turel, I. *Dalton Trans.* **2011**, *40*, 5188−5199.

(e) Kljun, J.; Bratsos, I.; Alessio, E.; Psomas, G.; Repnik, U.; Butinar, M.; Turk, B.; Turel, I. *Inorg. Chem.* **2013**, *52*, 9039−9052. (f) Bratsos, I.; Birarda, G.; Jedner, S.; Zangrando, E.; Alessio, E. *Dalton Trans.* **2007**, 4048−4058.
(20) Rilak, A.; Bratsos, I.; Zangrando, E.; Kljun, J.; Turel, I.; Bugarčić, Ž. D.; Alessio, E. *Dalton Trans.* **2012**, *41*, 11608−11618.
(21) Huang, W.; Qian, H. *J. Mol. Struct.* **2008**, *874*, 64−76.
(22) Bratsos, I.; Alessio, E. *Inorg. Synth.* **2010**, *35*, 148−152.
(23) Sullivan, B. P.; Calvert, J. M.; Meyer, T. J. *Inorg. Chem.* **1980**, *19*, 1404−1407.
(24) Ziessel, R.; Grosshenny, V.; Hissler, M.; Stroh, C. *Inorg. Chem.* **2004**, *43*, 4262−4271.
(25) Wasylenko, D. J.; Ganesamoorthy, C.; Kolvisto, B. D.; Henderson, M. A.; Berllnguette, C. P. *Inorg. Chem.* **2010**, *49*, 2202−2209.
(26) Gupta, N.; Grover, N.; Neyhart, G. A.; Singh, P.; Thorp, H. H. *Inorg. Chem.* **1993**, *32*, 310−316.
(27) Otwinowski, Z.; Minor, W. *Methods Enzymol.* **1997**, *276*, 307−326.
(28) Altomare, A.; Burla, M. C.; Camalli, M.; Cascarano, G. L.; Giacovazzo, C.; Guagliardi, A.; Moliterni, A. G. G.; Polidori, G.; Spagna, R. *J. Appl. Crystallogr.* **1999**, *32*, 115−119.
(29) Sheldrick, G. M. *Acta Crystallogr., Sect. A: Found. Crystallogr.* **2008**, *64*, 112−122.
(30) (a) Macrae, C. F.; Edgington, P. R.; McCabe, P.; Pidcock, E.; Shields, G. P.; Taylor, R.; Towler, M.; Van De Streek, J. *J. Appl. Crystallogr.* **2006**, *39*, 453−457. (b) Farrugia, L. J. *J. Appl. Crystallogr.* **1997**, *30*, 565. (c) Spek, A. L. *J. Appl. Crystallogr.* **2003**, *36*, 7−13. (d) Spek, A. L. *Acta Crystallogr., Sect. D: Biol. Crystallogr.* **2009**, *65*, 148−155. (e) Brandenburg, K.; Putz, H. *Diamond—Visual Crystal Structure Information System*, version 3.1; Crystal Impact GbR: Bonn, Germany, 2006.
(31) Bratsos, I.; Simonin, C.; Zangrando, E.; Gianferrara, T.; Bergamo, A.; Alessio, E. *Dalton Trans.* **2011**, *40*, 9533−9543.
(32) (a) Chatterjee, D.; Sengupta, A.; Mitra, A. *Polyhedron* **2007**, *26*, 178−183. (b) Patel, M. N.; Gandhi, D. S.; Parmar, P. A.; Joshi, H. N. *J. Coord. Chem.* **2012**, *65*, 1926−1936. (c) Papaefstathiou, G. S.; Sofetis, A.; Raptopoulou, C. P.; Terzis, A.; Spyroulias, G. A.; Zafiropoulos, T. F. *J. Mol. Struct.* **2007**, *837*, 5−14.
(33) (a) Nakamoto, K. *Infrared and Raman spectra of inorganic and coordination compounds*, 6th ed.; John Wiley & Sons, Inc.: Hoboken, NJ, 2009; Part B. (b) Rachford, A. A.; Petersen, J. L.; Rack, J. J. *Inorg. Chem.* **2005**, *44*, 8065−8075. (c) Rack, J. J.; Rachford, A. A.; Shelker, A. M. *Inorg. Chem.* **2003**, *42*, 7357−7359.
(34) (a) Gejji, S. P.; Hermansson, K.; Lindgren, J. *J. Phys. Chem.* **1993**, *97*, 3712−3715. (b) Miles, M. G.; Doyle, G.; Cooney, R. P.; Tobias, R. S. *Spectrochim. Acta, Part A* **1969**, *25*, 1515−1526.
(35) Heyns, A. M. *Spectrochim. Acta, Part A* **1977**, *33*, 315−322.
(36) (a) Takeuchi, K. J.; Thompson, M. S.; Pipes, D. W.; Meyer, T. J. *Inorg. Chem.* **1984**, *23*, 1845−1851. (b) Dovletoglou, A.; Adeyemi, S. A.; Meyer, T. J. *Inorg. Chem.* **1996**, *35*, 4120−4127. (c) Root, M. J.; Deutsch, E. *Inorg. Chem.* **1985**, *24*, 1464−1471.
(37) Wang, F.; Chen, H.; Parsons, S.; Oswald, I. D. H.; Davidson, J. E.; Sadler, P. J. *Chem.—Eur. J.* **2003**, *9*, 5810−5820.
(38) Miller, S. E.; House, D. A. *Inorg. Chim. Acta* **1991**, *187*, 125−132.
(39) Alessio, E.; Xu, Y.; Cauci, S.; Mestroni, G.; Quadrifoglio, F.; Viglino, P.; Marzilli, L. G. *J. Am. Chem. Soc.* **1989**, *111*, 7068−7071.
(40) (a) Sigel, H. *Pure Appl. Chem.* **2004**, *76*, 1869−1886. (b) Massoud, S. S.; Corfù, N. A.; Griesser, R.; Sigel, H. *Chem.—Eur. J.* **2004**, *10*, 5129−5137.
(41) Rilak, A.; Petrović, B.; Grgurić-Šipka, S.; Tešić, Ž.; Bugarčić, Ž. *Polyhedron* **2011**, *30*, 2339−2344.
(42) (a) Kunick, C.; Ott, I. *Angew. Chem., Int. Ed.* **2010**, *49*, 5226−5227. (b) Meggers, E.; Atilla-Gokcumen, G. E.; Gründler, K.; Frias, C.; Prokop, A. *Dalton Trans.* **2009**, 10882−10888.